doi: 10.13133/2280-6148/19184 *Journal of Mediterranean Earth Sciences 17 (2025), 71-94*

J M E S **Journal of Mediterranean Earth Sciences**

A new turbidite facies-tract scheme including supercritical and hydraulic jump facies: interactions between basin morphology and criticality

Roberto Tinterri *

Dipartimento di Scienze Chimiche, della Vita e della Sostenibilità Ambientale, Unità di Scienze della Terra, Università di Parma, Parma, Italy
** Corresponding author: roberto.tinterri@unipr.it*

ABSTRACT - Studies of tectonically confined turbidite systems in Mediterranean-type foreland basins have shown that these deposits can be dominated by supercritical flows, which can transform into subcritical and/or transitional (mud–sand) flows. In these confined turbidite systems, supercritical flows tend to be favored by lateral confinements parallel to the paleocurrents. In contrast, flow decelerations are favored by morphologies transversal to paleocurrents, e.g., slope breaks or adverse slopes that can vary in scale from regional tectonic structures to depositional features such as thick mass-transport complexes and lobes. This evidence, together with the growing knowledge of supercritical flow processes and structures that has occurred over the last fifteen years, has led to the formulation of a new facies scheme that takes into account the relationship between basin geometry and criticality. This has also prompted a revisiting of the concept of efficiency, where the type of facies tract does not only depend on the flow behavior but also on the basin size and morphology.

Keywords: supercritical flow; hydraulic jump; facies tract; turbidites; basin morphology.

Submitted: 30 October 2025 - Accepted: 08 December 2025

1. INTRODUCTION

The rationale behind this work is to discuss the new facies-tract scheme by Tinterri (2025), trying to focus on some aspects of the facies related to supercritical flows and hydraulic jumps as indicators of different-scale basin morphologies.

Growing evidence from field and subsurface data shows clearly that the degree of basin confinement and geometry, as well as various scales of basin-floor morphologies, are the major controlling factors of flow evolution and type of facies tract (e.g., Pickering and Hiscott, 1985; Remacha et al., 2005; Muzzi Magalhaes and Tinterri, 2010; Tinterri and Muzzi Magalhaes, 2011; Tinterri and Tagliaferri, 2015; Tinterri and Piazza, 2019; Gallicchio et al., 2023; Catto et al., 2024). For example, basin–confining morphologies parallel or perpendicular to the paleocurrents may favor or hinder flow evolution, respectively, and this controls not only flow dynamics but also flow criticality, i.e., whether the flow is supercritical or subcritical with the possibility to form a hydraulic jump (Tinterri, 2025). At a regional scale, these morphologies can depend on tectonic setting and tectonic structure orientation, which, in turn, can control small–scale depositional features that can form morphological barriers. Hence, the new general facies–tract scheme proposed by Tinterri (2025), which attempts to relate lateral-vertical distribution of supercritical, hydraulic jump, and subcritical structures with basin morphologies, may greatly help identify syndepositional basin tectonics and basin configurations. Consequently, this new scheme is particularly suitable for turbidite systems deposited in confined and narrowed foredeep and wedge top basins where the degree of confinement and basin geometry favor deceleration and transformation of supercritical bipartite flows. Thus, in this discussion central becomes also the concept of sediment transport efficiency that is related not only to the flow characteristics but also to basin type, tectonic setting, degree of basin confinement, and basin–floor morphology.

From this point of view, to discuss this new facies-tract scheme, the sedimentary structures and processes related to supercritical flows and the role of hydraulic jumps are first examined.

2. FLOW CRITICALITY IN TURBIDITE FACIES SCHEMES

The first facies–tract scheme that discusses the flow criticality of turbidite facies is that by Mutti (1992), (see also the updated version by Mutti et al., 2003). It covers a wide spectrum of turbidite facies and processes, strongly influenced by Lowe (1982), who introduced four main groups of facies, each one characterized by a well-defined dynamic grain-size population, recording the deposits of four different types of sediment gravity flows evolving downcurrent (Fig. 1 A,B). This facies–tract scheme, characterized by nine facies (F1-F9), is formed by the progressive transformation of a parent debris flow into a subcritical high-to low-density turbidity current via a supercritical gravelly high-density turbidity current (Fig. 1 B,C). From this point of view, the sedimentation phases by Lowe (1982) (traction, traction carpets, and suspension sedimentation) are associated with decelerating supercritical flows that undergo a hydraulic jump to form F6 facies. The concept of sedimentation phases by Lowe (1982) is here considered fundamental to understand the passage from a supercritical to subcritical regime (see Fig. 1A). This is also incorporated into depositional models by Hiscott and Middleton (1979) and Massari (1984) that interpreted the crudely laminated to massive coarse-grained sandstones (B1 facies by Mutti and Ricci Lucchi, 1972) overlain by tractive structures (B2 facies by Mutti and Ricci Lucchi, 1972) to be related to the deceleration of supercritical high-density turbidity currents.

After Mutti (1992), one of the few schemes that consider flow criticality is from Postma and Cartigny (2014), although a large number of other works dealing with theoretical considerations, direct measurements of turbidity currents, experimental works, and numerical modelling have shown that density currents and high-density stratified flows can be dominated by supercritical conditions due to the effect of reduced density contrast (e.g., Postma et al., 2009, 2016; Cartigny et al., 2014; Dorrell et al., 2016; Hage et al., 2018; Slootman and Cartigny, 2020; Vendettuoli et al., 2019; Pohl et al., 2020, 2022; Scacchia et al., 2022a, 2024; Sequeiros et al., 2026 with references). In this classification, Postma and Cartigny give particular emphasis to stratified (bipartite) flows and cyclic–step dynamics, in which the flow, supercritical and erosive down the lee face, decelerates in the trough through a hydraulic jump (Fig. 2A, B). Consequently, the depositional style of cyclic steps may be expected to be characterized by massive facies followed by various types of crude lamination that reflect an increase in flow velocity and a decrease in the sediment fallout rate (Fig. 2B). This model highlights the importance of the recognition of hydraulic–jump facies (i.e., Ta with flame structures in Fig. 2A) to discriminate between supercritical and subcritical deposits. The latter point is particularly emphasized by Mutti (2023), where a key role is given to the facies produced by major flow transformation, such as hydraulic jumps. These facies types distinguish the deposits related to inertia flows and supercritical high-density turbidity currents from Bouma-like deposits associated with subcritical low-density turbidity currents.

In this way, the facies tract scheme by Tinterri (2025) takes into account all these considerations trying to link the facies scheme by Postma and Cartigny (2014), who classify turbidites according to facies sequences (associations) that reflect specific flow dynamics with the facies-tract scheme of Mutti et al. (2003), which is based on the downslope evolution of a decelerating and depletive flow. The desire to link both schemes derives from a great number of foreland basin field studies that highlight to demonstrate the need for a new scheme that includes depositional modes produced by decelerating, supercritical turbidity currents relevant for tectonically controlled basin configurations. The studies carried out in the last twenty years on turbidite deposits in confined and narrowed foredeeps and wedge-top basins have shown that, in these strata, sedimentary structures indicating supercritical flows and their transformation into subcritical flows are quite common (e.g., Demko et al., 2014; Hoyal et al., 2014; Postma et al., 2014, 2021; Postma and Kleverlaan, 2018; Pickering and Hiscott, 2016; Cornard and Pickering, 2019, 2020; Cornard et al., 2025; Tinterri et al., 2017, 2020; Tinterri, 2025). In these types of turbidite systems, flow decelerations related to the basin confinement and morphology must favor especially the formation of stratified (bipartite) flows and efficient decoupling flow processes. The latter implies the formation of high-density, basal flows dominated by decelerating supercritical flows that may form hydraulic jumps and the bypass of overriding, subcritical turbulent flows able to produce different types of traction and traction-plus-fallout structures (see Tinterri and Muzzi Magalhaes, 2011; Tinterri, 2025). In these settings, hydraulic jump, fundamental for separating supercritical and subcritical processes, is generally triggered by different scale morphologies and is always characterized by a well-determined facies (e.g., Postma et al., 2009; Tinterri, 2025). For this reason, a review of the processes acting at this transition is given in the next section.

3. CRITICALITY, FLOW REGIMES AND HYDRAULIC JUMPS

3.1. SUPERCRITICAL CONDITIONS OF DENSITY FLOWS

Criticality and flow regimes are distinct concepts, though often related. Criticality in turbidity currents is governed by the densimetric Froude number $FR_d=U^2/g'h$, where U is the current velocity, $g'=g\Delta\rho/\rho_2$ is the acceleration due to gravity to account for density stratification in the vertical, and h is the current thickness. Supercritical flows occur when $Fr_d>1$ and antidunes, chute and pools and cyclic steps are stable; conversely, subcritical flows occur when $Fr_d<1$ and ripples and dunes are stable. In critical condition ($Fr_d=1$), the passage from supercritical flows

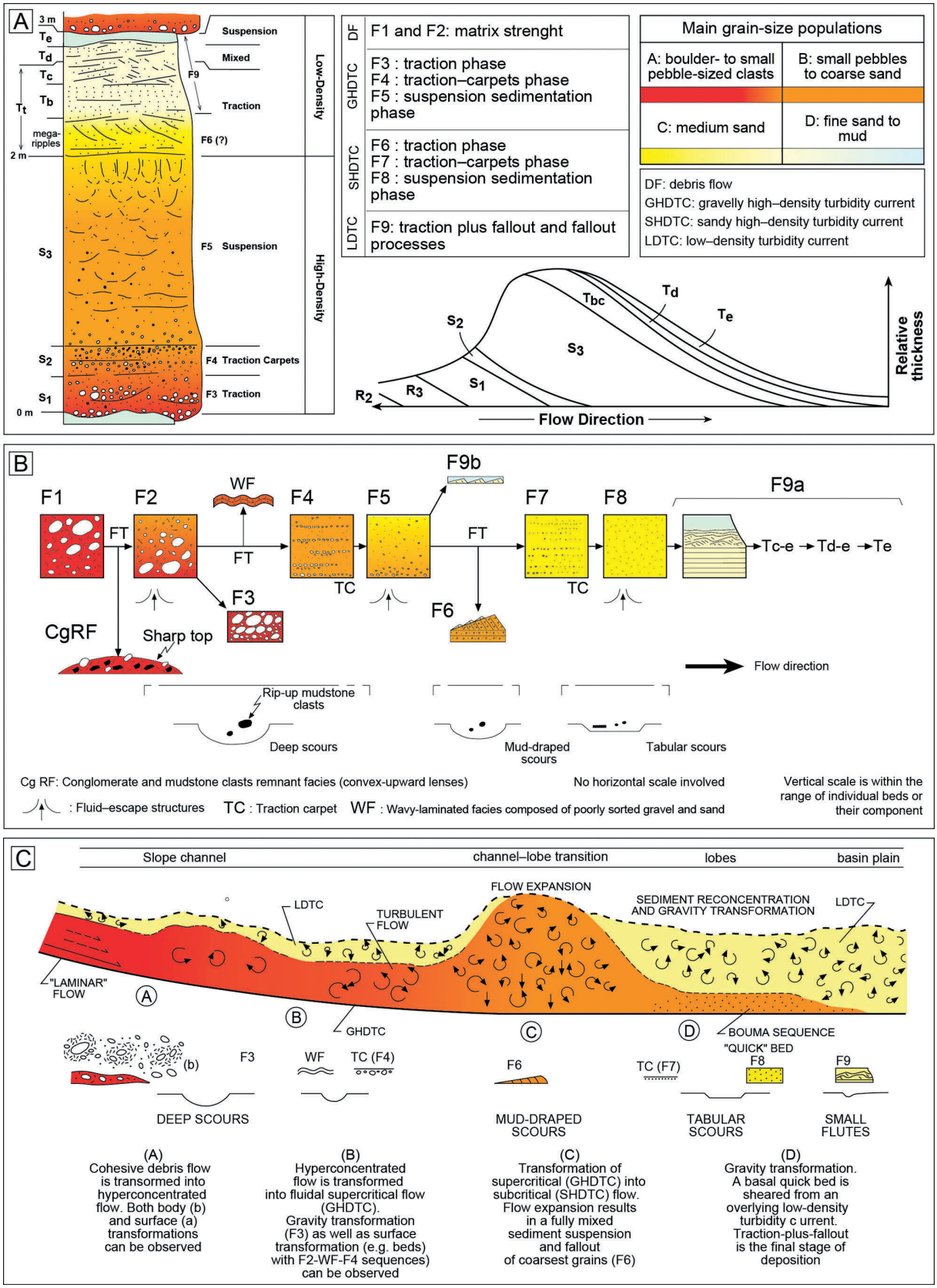

Fig. 1 - A) Ideal deposit of a sandy high-density turbidity current from Lowe (1982), showing high-density (S1-3) and low-density (Tt, Tde) divisions; on the right, a diagram showing downslope evolution of a turbidite deposit. A comparison between the F1–9 facies by Mutti (1992) and the depositional phases by Lowe (1982) is also shown; B) Classification scheme of turbidite facies (F1–9) by Mutti (1992) (for an updated version see Mutti et al., 2003). C) Diagram showing the main flow transformations during the downcurrent evolution of a sediment–gravity flow. This diagram is associated with the facies tract shown in B. Figure from Tinterri (2025).

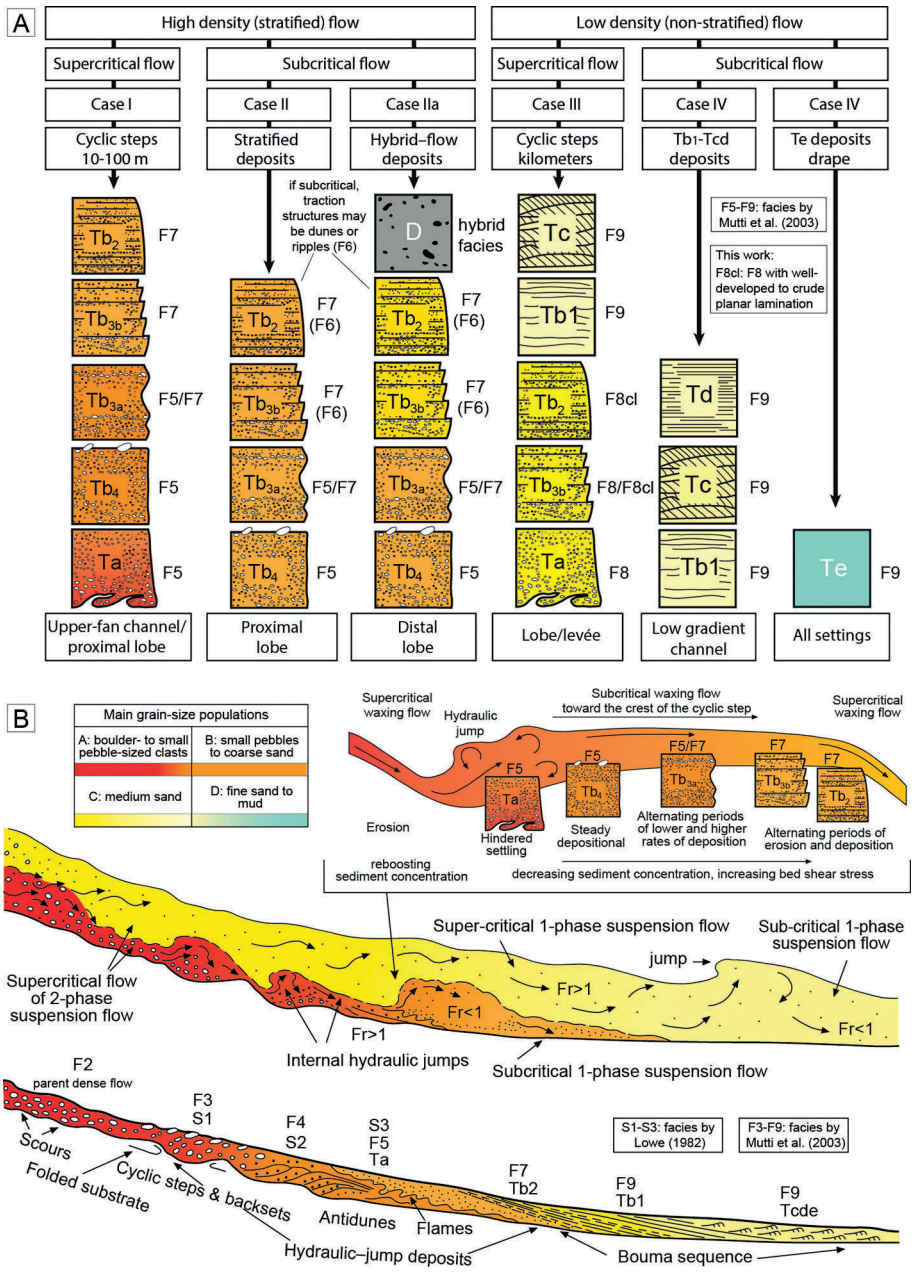

Fig. 2 - A) Suites of facies characteristics (facies associations) related to flow dynamics (cases I–IV) and depositional sub-environments. Flow is from left to right (from Postma and Cartigny, 2014). B) Above, cyclic step facies (note the facies change along the stoss side). Below, diagrams describing flow transformations from supercritical to subcritical through an internal hydraulic jump leading to the development of Bouma Ta with flame structures (modified from Postma, 2011). To be noted are the analogies with the diagram in Figure 1C. Figure from Tinterri (2025).

into subcritical flows can occur through a hydraulic jump.

Flow regimes, on the other hand, describe a physical pattern or a structure of a flow's motion. In particular, upper and lower flow regimes (characterized by distinct bedforms) describe different sedimentary conditions based on flow velocity and the in-phase relation between flow surface and bedforms. The lower flow regime includes ripples and dunes and has slower flow speeds, where the bedforms are out of phase with the water surface, while upper flow regime occurs at higher flow speeds and includes planar laminae, antidunes, and chutes and pools, where the surface waves are in phase with the bedforms (Fig. 3). In particular, plane and parallel laminae, although can be considered of upper flow regime because are in phase with the water surface, they usually form under subcritical flow conditions (see Fig. 3). Conversely, cyclic steps (stable at very high Froude number) are characterized by an alternation of supercritical and subcritical conditions separated by hydraulic jumps where flows are out of phase in the subcritical part and in phase in the supercritical part. In this case, as suggested by Slootman (2020), a third flow regime could be introduced that may be indicated as an upper-upper flow regime (Fig. 3).

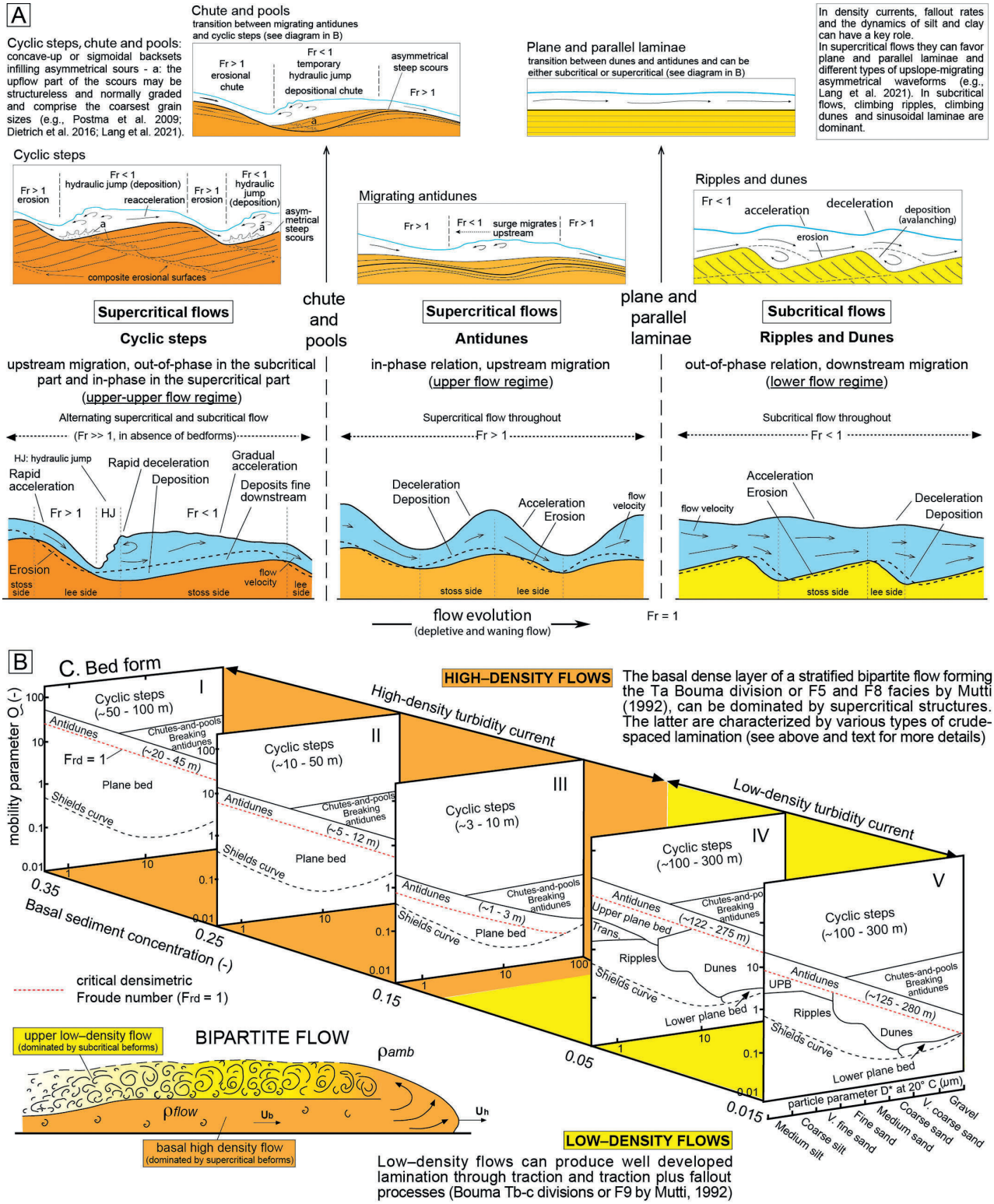

Fig. 3 - A) Diagrams describing supercritical and subcritical bedforms in relation to flow criticality and flow regimes (modified from Slootman and Cartigny, 2020 and Slootman, 2020). B) Bedform stability diagram in relation to an increase in the fallout rate (modified from Cartigny and Postma, 2016). To be noted the type of bedforms characterizing the high-density basal layer and upper turbulent layer of a bipartite flow (modified from Tinterri, 2025).

Many works have shown that upper flow regime structures, described by the classic works by Simons et al. (1965), Harms and Fahnestock (1965), Middleton (1965), Walker (1967), Jopling and Richardson (1966) and Hand (1974), are much more common in the geological record than previously thought (e.g., Alexander et al.,

2001; Bridge, 2003; Fielding, 2006; Tinterri, 2011). In the last fifteen years, indeed, there has been an increase in studies on upper–flow–regime structures, including the proposal of new bedforms stability diagrams (e.g., Cartigny et al., 2014; Cartigny and Postma, 2016; Fedele et al., 2016; Slootman and Cartigny, 2020, Slootman et al., 2021; Sequeiros et al., 2026 with references) considering the role of hydraulic jumps and cyclic–step dynamics on channel–lobe transition (e.g., Postma et al., 2009, 2014, 2016, 2021; Hamilton et al., 2015; Dorrell et al., 2016; Lang et al., 2017; Hage et al., 2018; Postma and Kleverlaan, 2018; Ono and Plink-Björklund, 2018; Ono et al., 2021; Cornard and Pickering, 2019, 2020; Pohl et al., 2020, 2022; Tinterri et al., 2020; Grundvag et al., 2025).

In general, supercritical conditions can be expected to be more common in density currents than in open-channel flows (Menard, 1964; Middleton, 1966; Komar, 1971; Hand, 1974; Mutti and Normark, 1987; Piper and Normark, 2001). FR_d, indeed, is the ratio of inertial to gravitational forces modified by the effects of buoyancy due to the introduction of the term $\Delta\rho/\rho_2$ (where ρ_2 is the flow density and $\Delta\rho=\rho_2-\rho_1$ is the density contrast between the flow and the ambient fluid). Buoyancy reduces the influence of gravity and significantly slows the propagation of the shallow gravity waves in the density interfaces (i.e., the denominator of Fr_d). This means that, in density currents, supercritical conditions can be very common, even at low velocities (Komar, 1971; Hand, 1974; Postma et al., 2009; Fricke et al., 2015). For example, analyzing the velocity and concentration of a wide range of experimental and natural density flows, Sequeiros (2012) found that a slope with an angle of $\alpha \approx 0.45°$ is sufficient to reach supercritical conditions.

Consequently, in a density-stratified flow, the basal high-density part can be particularly favourable in order for supercritical bedforms to be generated, and high fallout rates can be an important control factor of the type of supercritical bedforms (e.g., Lang et al., 2021a). The diagram in Figure 3, for example, show that, in waning flows, a progressive increase in the basal–layer density due to a fallout-rate increase produces a progressive turbulence suppression that causes an expansion of the upper–flow regime structures and a progressive disappearing of stability fields of the tractive structures, i.e., ripples and dunes (Cartigny and Postma, 2016; see also Lowe, 1988). Subcritical bedforms are indeed dependent on low-density turbulent flows that allow flow separations necessary for avalanching processes (Fig. 3). However, it is interesting to note that, with a progressive increase in the sediment concentration, upper flow regime bedforms are characterized by a progressive increase in the stability field of planar laminae and a concomitant subtle decrease in those of antidunes, chute and pools and cyclic steps (Fig. 3). This evidence may be explained with the necessity of turbulence development for allowing a hydraulic jump in supercritical bedforms which is not necessary for plane and parallel laminae. This evidence was well highlighted by Lowe (1988) that for high flow densities due to high suspended load fallout rates, plane and parallel laminae (Tb Bouma division) and massive facies (Ta Bouma division or S3 Lowe division) are stable.

In the rock record, indeed, supercritical deposits are characterized by different types of centimeter-thick spaced and crude lamination, which are thought to reflect high basal sediment concentrations (Hiscott and Middleton, 1979; Hiscott, 1994; Sohn, 1997; Talling et al., 2012; Cartigny et al., 2013), while hydraulic jumps can be recorded by massive facies with water escape and flame structures indicating drastic flow decelerations (e.g., Postma et al., 2009), that are often triggered by morphologies transverse to the paleocurrents (Tinterri, 2025). For this reason, a review of the processes that can occur at the transition between supercritical and subcritical flow and consequently on the dynamics of the hydraulic jumps, will be done in the next section.

3.2. TRANSITION BETWEEN SUPERCRITICAL AND SUBCRITICAL REGIMES AND HYDRAULIC JUMP

The recent work by Tinterri (2025) has highlighted as the transition from supercritical to subcritical flows can occur in different ways and can involve a hydraulic jump or not, and how the dynamics of this passage can be triggered by slope-break and counter-slope basin–floor morphologies at different scale (Fig. 4). In particular, in tectonically confined turbidite systems, supercritical flows can be favoured by lateral confinements parallel to the paleocurrents which help to maintain the flow energy, while flow decelerations which may form hydraulic jumps, are favoured by morphologies transversal to the paleocurrents, e.g., slope breaks or adverse slopes that can vary in scale from regional tectonic structures to depositional features such as thick mass-transport complexes and lobes.

In supercritical bedforms and thus at relatively small scales, hydraulic jumps are triggered by counterslopes associated with the stoss sides (Fig. 4A). From unstable antidunes to cyclic steps passing through chute and pools, hydraulic jumps become more and more ordered and cyclic (e.g., Cartigny et al., 2014). In particular, in chute and pools and cyclic steps, the flow at the hydraulic jump can form massive deposits in asymmetrical scours with backset geometries and then accelerates again towards the crest to form tractive structures (see Fig. 3; see also Postma et al., 2014; Hage et al., 2018; Ono and Plink-Bjorklund, 2018; Lang et al., 2021a). Furthermore, the wavelength of cyclic steps depends on the distance that the flow needs to become critical again after the hydraulic jump, and in stratified flows, where only the dense basal layer interacts with the bed, the size of the cyclic steps is relatively limited, ranging from tens to hundreds of meters (Cartigny et al., 2011; Kostic, 2011; Cartigny and Postma, 2016; Postma et al., 2021).

In case of a slope break in a channel–lobe transition, a supercritical flow may switch to a subcritical flow through different types of hydraulic jumps characterized by an abrupt increase in flow depth and a decrease in

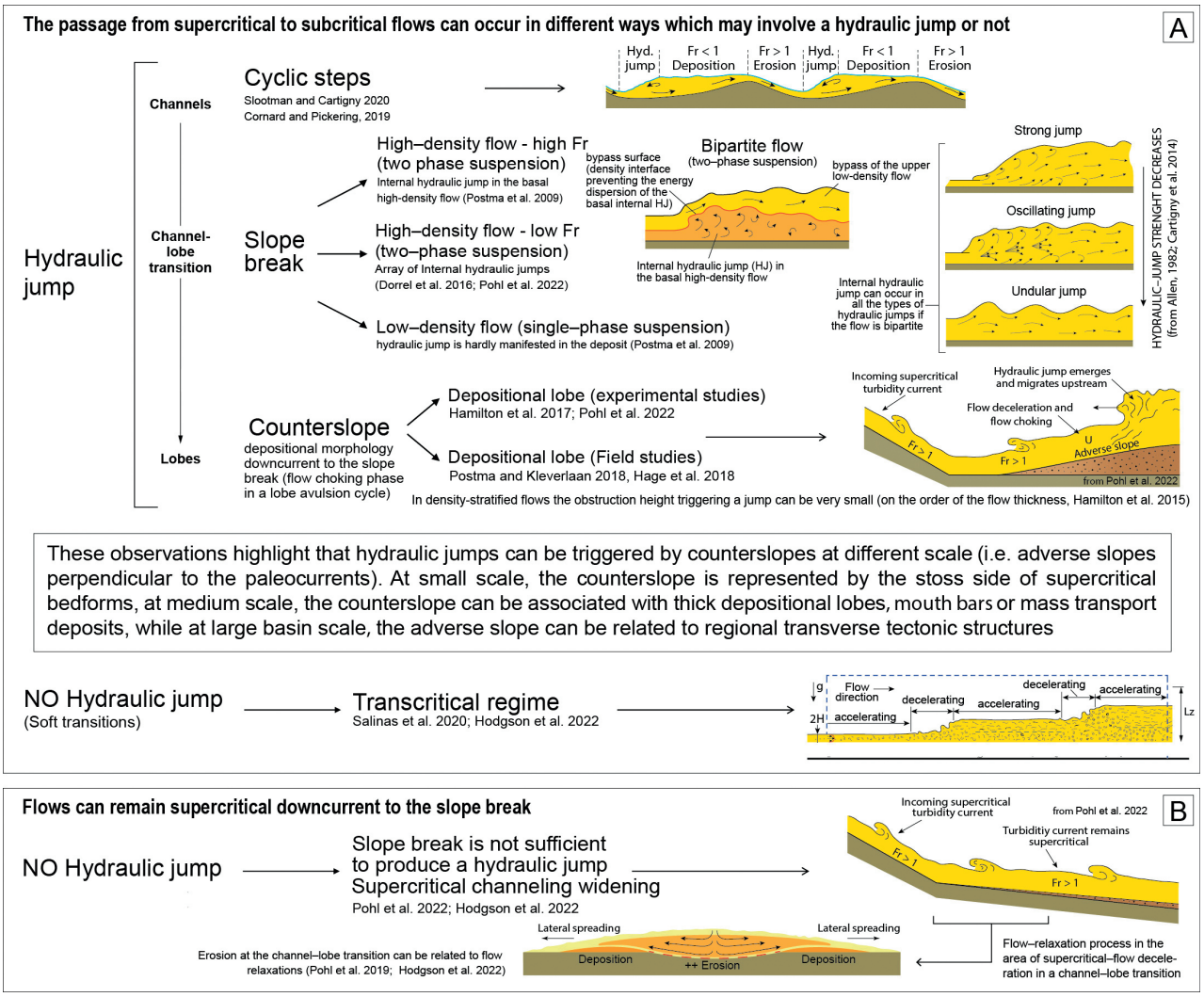

Fig. 4 - A) Schematic summary of the processes that can occur at the transition between supercritical and subcritical flows, pointing out that this transition can also occur without a hydraulic jump. B) Processes indicating how flows can pass a slope break while remaining supercritical. The diagrams also give the main references (modified from Tinterri, 2025).

flow velocity, accompanied by substantial energy loss (e.g., Komar, 1971; Garcia and Parker, 1989; Dorrel et al., 2016). The type of hydraulic jump depends on the ratio of the outgoing subcritical-flow depth behind the jump and incoming supercritical-flow depth in front of the jump (conjugate depths) and can be related to the energy loss (ΔH) over the hydraulic jump (Fig. 4A; see Cartigny et al., 2014 for more details). Evidence of hydraulic jumps triggered by slope breaks comes not only from field examples (e.g., Mutti and Normark, 1987, 1991; Mutti et al., 2003; Ito et al., 2014; Hofstra et al., 2015; Henstra et al., 2016; Cunha et al., 2017) and seafloor data (e.g., Wynn et al., 2002; Hodgson et al., 2022), but also from experimental data, numerical simulations and real-world flow measurements (e.g., Komar, 1971; Garcia and Parker, 1989; Garcia, 1993; Sumner et al., 2013; Dorrel et al., 2016).

In many other experimental and numerical works, however, hydraulic jumps are not triggered by the slope break, but by an adverse slope downstream of the slope break, which produces significant deceleration, chocking of the flow and an upcurrent migration of the hydraulic jump (e.g., Pohl et al., 2020, 2022; see also Fig. 4A). In other words, hydraulic jumps are produced by different scale counterslopes ranging from structural highs within the basin to relatively small, critical step heights associated with depositional morphologies (i.e., lobes or mouth–bar deposits) formed downstream of the slope break (e.g., Tinterri, 2025). For example, at a medium scale, Hamilton et al. (2015, 2017), in their experiments on autogenic avulsion cycles on submarine fans, show that the deposition of a mouth bar at a channel outlet represents an obstacle to flows leaving the channel outlet, which started to choke up, culminating in a hydraulic jump that migrates upcurrent. Similar interpretations based on field data come from Postma and Kleverlaan (2018), Postma et al. (2021). In these studies, the formation of a hydraulic jump is interpreted

to occur at a later stage of a depositional–lobe formation, characterized by sediment accretion and flow choking, rather than a direct result of an interaction with a slope break (Fig. 4A). This interpretation is particularly valid in tectonically confined basins, where deceleration and fallout rates favor the formation of relatively thick and amalgamated lobes (e.g., Tinterri and Tagliaferri, 2015; Tagliaferri et al., 2018; Piazza and Tinterri, 2019, 2020; Pizzati and Tinterri, 2023; Catto et al., 2024; Tinterri, 2025). Conversely at large basin scale, flow decelerations and hydraulic jumps can be triggered by basin margins (e.g., Kneller and McCaffrey, 1999; Amy et al., 2004, 2007; Tinterri et al., 2017; Cunha et al., 2017; Tinterri and Civa, 2021), and structural highs transverse to the paleocurrents (e.g., Howlett et al., 2019; Tinterri et al., 2016, 2022; Tinterri, 2025). Regarding these points, it is important to stress that in density-stratified flows the height of the obstacle, able to trigger a hydraulic jump, can be very small (i.e., on the order of flow thickness, Hamilton et al., 2015; Postma et al., 2016; see also Fig. 4A).

These considerations, therefore, point out the importance of medium- and large-scale adverse slopes such as depositional lobes or MTCs and basin-scale counterslopes, which, as they are generally associated with transversal tectonic structures, can trigger important flow transformations and hydraulic jumps (e.g., Tinterri et al., 2020, 2022; see Fig. 4A). In these cases, the hydraulic jump in turbidity currents or stratified (bipartite) density flows can occur internally within the high-density basal layer, whereas the low-density uppermost component of the flow can bypass above it (Figs. 4A, 5A). In this case, since the hydraulic jump occurs in the high-density basal layer of the flow and thanks also to the presence of a density interface, mixing driven by turbulent expansion, recirculation, and deceleration of the flow is contained, and entrainment of ambient water is reduced (Postma et al., 2009; Dorrell et al., 2016).

In stratified density flows, various scenarios of sediment deposition can exist (see Fig. 4A). Dorrell et al. (2016) showed that, in stratified flows with low FR_d, the increase in turbulence due to internal hydraulic jumps may enhance the sediment transport downstream of the jump. Conversely, well-developed bipartite (two-phase suspension) flows with high-velocity supercritical basal layers cause vigorous erosion and liquefaction of the substrate at the jump locality to produce flame structures and rip-up clasts, which are trapped in structureless, coarse-tail-graded deposits typical of the Bouma Ta division (Postma et al., 2009). In their experiments, these authors showed the basal high-density layer passed the hydraulic jump and expanded vigorously, resulting in strong, upward disruption of the top of the substrate, which was fully suspended by the flow; subsequently, the dense suspension underwent rapid deposition to form, under conditions of virtually no lateral shear, a structureless bed (Fig. 5A). The rapid drop in velocity of the basal layer at the hydraulic jump significantly increases the pressure above the bed to form flame structures at the base of structureless beds, while the pressure in the upper low-density layer remains unchanged, and the layer can bypass and rework the top of the massive bed (Fig. 5A). In this setting, the hydraulic jump is also seen to move upcurrent, and its associated massive deposits can have a backset geometry (e.g., Hamilton et al., 2015; Hage et al., 2018; Postma and Kleverlaan, 2018).

However, various numerical and experimental modelling studies suggest that the passage from supercritical to subcritical regimes can also occur without hydraulic jumps even in the presence of a slope break (e.g., Garcia, 1993; Kostic and Parker, 2006; Gray et al., 2005; Salinas et al., 2020; Lang et al., 2021b; Pohl et al., 2022; see Fig. 4A). In particular, Salinas et al. (2020) show that this transition can occur through an intermediate transcritical regime where intermittent cascading interfacial instabilities appear, while Pohl et al. (2019) show that the widespread occurrence of scours at the channel mouth can be explained with a new flow mechanism called flow relaxation rather than hydraulic jump (Fig. 4 A,B; see also Wilkin et al., 2023). These apparently contrasting results show that both flow dynamics and erosional–depositional signals of a turbidity current crossing a slope break or an adverse slope can still be a subject of debate, and despite the variability of processes highlighted by the experimental data, a better understanding of the transition from supercritical to subcritical flows must rely on careful integration with field data (e.g., Tinterri, 2025).

4. A GENERAL FACIES TRACT FOR TURBIDITES CONTROLLED BY BASIN MORPHOLOGIES: THE ROLE OF SUPERCRITICAL HIGH-DENSITY FLOWS, HYDRAULIC JUMPS, AND BYPASSING FLOWS

4.1. INTRODUCTION

The facies scheme by Tinterri (2025) is based on the concept of genetic facies tract by Lowe (1982) and Mutti (1992), which is defined as an association of genetically related facies types which record, within each considered system, the downstream evolution of a sediment gravity flow. The ideal facies tract is recorded by a bed deposited by a single sediment gravity flow undergoing transformations during its basinward motion. In these terms, the concept of gravity-flow facies can be applied to a specific depositional division within a bed (i.e., lamina or laminaset, *sensu* Campbell, 1967; see Fig. 5). Consequently, within a bed, the vertical facies association (i.e., the facies sequence) represents how the flow conditions change in time at a fixed location along the path of the flow; the horizontal facies association, or simply facies association (i.e., the facies tract), records how the flow conditions change in space through successive flow transformations (Fig. 5). This approach implies that, for each considered turbidite system, facies tracts must be established within a time-equivalent interval based on detailed stratal correlation patterns.

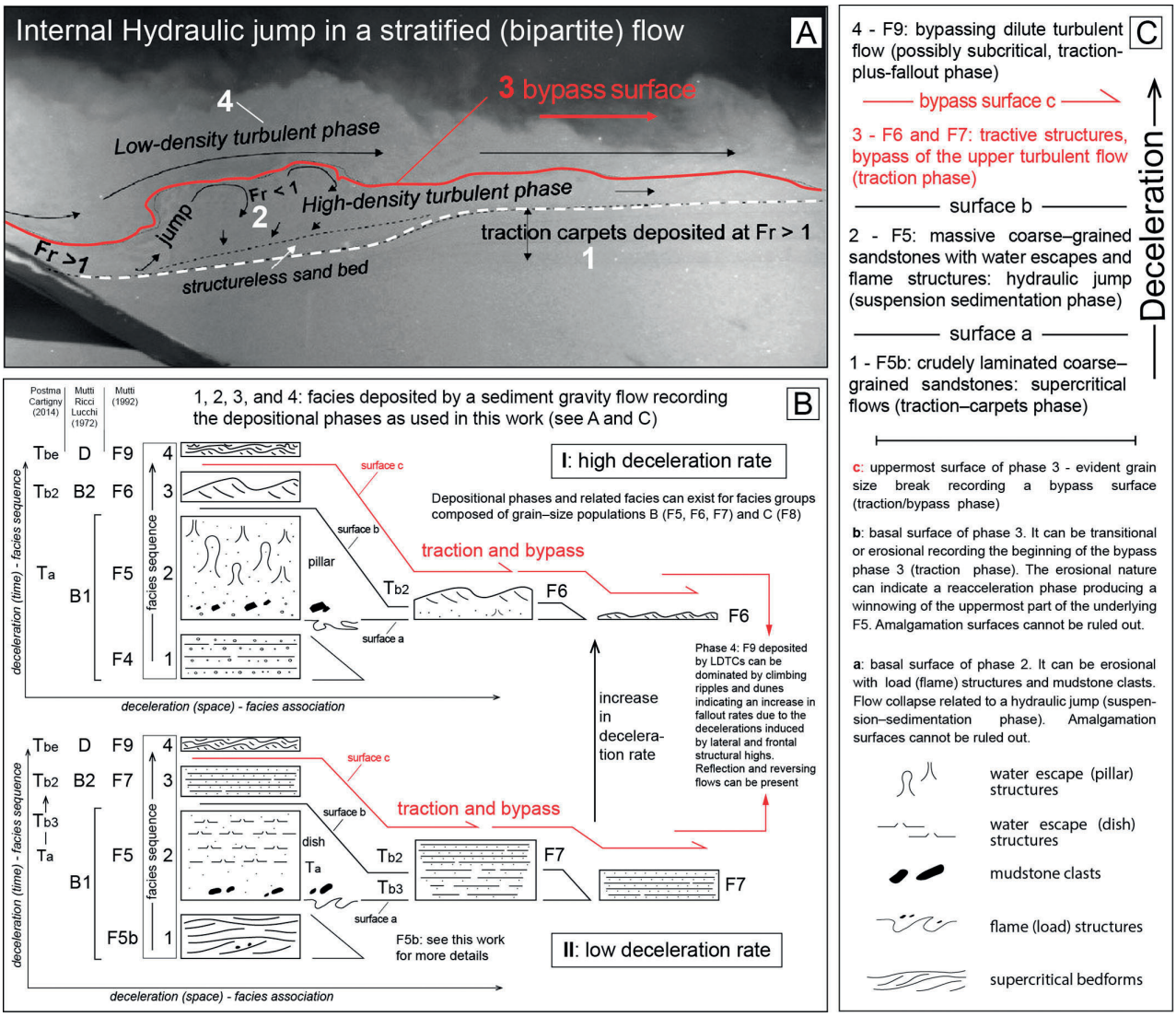

Fig. 5 - A) Dynamic phases characterizing a hydraulic jump of a two-phase (bipartite) particulate density flow (modified from Postma et al., 2009). B) Diagram illustrating the facies, facies sequences, and dynamic phases shown in A. The nomenclature of the facies schemes by Mutti (1992), Mutti and Ricci Lucchi (1972), and Postma and Cartigny (2014) are also shown. C) Explanation of the four dynamic phases and their boundary surfaces characterizing the transition from supercritical to subcritical flow as shown in A and B. Figure from Tinterri (2025).

In particular, as mentioned above, the facies tract scheme by Tinterri (2025) is based on the tentative link between the concepts by Postma and Cartigny (2014) who classify turbidites according to facies sequences (associations) reflecting specific flow dynamics, and the facies tract scheme by Mutti et al. (2003) which is based on the downslope evolution of a decelerating and depletive flow. The facies tract scheme by Tinterri (2025), however, is carefully calibrated through a great number of field data deriving from many turbidite systems in tectonically confined settings. In these types of turbidite systems that can be consistent with the supercritical fans by Demko et al. (2014) and mixed depositional systems by Mutti et al. (2003), the degree of confinement is controlled not only by lateral structural highs (i.e., parallel to the paleocurrents) that may favor energy conservation and supercritical flows but also by transverse tectonic structures (i.e., perpendicular to the paleocurrents), which, by forming important regional slope breaks and counter-slopes, can induce flow decelerations and flow-regime changes.

In these settings, high-gradient sandy turbidity currents can produce various types of traction carpets, crude laminations, and traction structures indicative of flow concentration and flow criticality (Fig. 5; Cartigny et al., 2013; see also Tinterri and Muzzi Magalhaes, 2011). Conversely, flow decelerations, especially if able to produce hydraulic jumps, can form massive sandstones with flame structures, mudstone clasts, and water escape structures derived from the collapse of the suspended load, thus recording a suspension-sedimentation phase (Postma et al., 2009, 2014; Tinterri, 2025).

A key point of the facies tract scheme by Tinterri (2025)

is that flow transformations and changes induced by basin morphology can be recorded by depositional phases conceptually similar to those introduced by Lowe (1982) (see also Hiscott and Middleton, 1979; Massari, 1984; Mutti, 1992). Their vertical or downstream order within a bed or a bedset can give important information on the predominance of supercritical flows that are especially enhanced by lateral confinements or on different degrees of flow decelerations that are more related to transverse morphologies. The model of figure 5 by Tinterri (2025), for example, illustrates the dynamic phases and related facies sequences characterizing a flow deceleration of a two-phase (bipartite) particulate density flow that can produce a hydraulic jump. In this figure, Facies 1 records a phase of traction-plus-fallout from supercritical flows (when associated with up-current-dipping laminae), while Facies 2 records a hydraulic-jump phase. Facies 3 is characteristic of bedforms produced by traction and records the bypass of subcritical low-density turbidity currents. The tail of these currents deposits a fine-grained Tbe division (Facies 4; see Fig. 5). The four facies types record four depositional phases that are well consistent with the experimental model by Postma et al. (2009), which shows that a supercritical flow can decelerate through a hydraulic jump to produce the collapse of a large part of the suspended sediment load and the bypass of an essentially subcritical upper dilute turbulent flow (Fig. 5A). Therefore, the facies sequences shown in Figure 5B can be explained by a vertical stacking of facies and thus depositional phases different from that proposed by Lowe (1982), as discussed by Hiscott and Middleton (1979) and Massari (1984) (see also Mutti et al., 2003; Kneller and McCaffrey, 2003; Tinterri and Muzzi Magalhaes, 2011).

In essence, the type of lateral and vertical stacking of these depositional phases and related facies can be indicative of the type of basin morphology that can control the dynamics and evolution of the turbidity currents. This evidence can be considered another key point on which is based the facies tract scheme by Tinterri (2025).

4.2. GENERAL FACIES-TRACT SCHEME

In figure 6, the general facies-tract scheme by Tinterri (2025) can be observed (see also Tab. 1). The scheme describes the evolution of a decelerating single supercritical sediment gravity flow and resultant deposits whose evolution is controlled by flow decelerations induced by transverse morphologies. This facies tract scheme is mainly based on field data coming from tectonically controlled foreland basins in the Alps, Apennines, and Pyrenees (see Tinterri, 2025, his table 2 for more details).

The new facies-tract scheme maintains the names and general meaning of the scheme developed by Mutti et al. (2003) as much as possible. The rationale behind the genetic scheme is based on two assumptions. Firstly, turbidity currents are bipartite flows consisting of a high-density basal layer moving faster and ahead of a more dilute upper turbulent flow (Sanders, 1965; Ravenne and Beghin, 1983; Postma et al., 1988; Mutti et al., 1999, 2003, 2009; Tinterri et al., 2003). Secondly, this facies scheme captures the dynamics associated with the deceleration of the basal dense layer and the bypass of the upper turbulent flow (e.g., Tinterri and Muzzi Magalhaes, 2011; Tinterri and Tagliaferri, 2015).

It shows four dynamic phases, discussed above (i.e., 1, supercritical flow; 2, suspension sedimentation/collapse and possible hydraulic jump; 3, bypass; and 4, bypassed flow) and associates them with the four dynamic grain-size A–D populations (see Fig. 6 and Tab. 1).

However, it is important to underline that the different vertical and lateral stacking of depositional phases and related facies may also be indicative of one basin configuration rather than another; in other words, the predominance of one facies or facies sequence rather than another can be directly associated with the different types of morphologies that can characterize the basin at different scales. For example, the predominance of supercritical and bypass phases rather than deceleration and hydraulic jump phases can be indicative of confined settings, like channels or narrow portions of the basin laterally confined by tectonic structures elongated parallel to the paleocurrents; conversely, the predominance of deceleration phases, which can produce hydraulic jumps, may be indicative of morphological barriers perpendicular to the paleocurrents represented by important transverse tectonic structures or by thick depositional features such as MTCs and particularly thick depositional lobes (see Tinterri et al., 2020; Tinterri, 2025).

The facies tract in figure 6 is characterized by four groups of facies, A through D, each one associated with a dominant dynamic grain-size population. Grain-size population A dominates the initial parent flow and its transformation into a bipartite high-density turbidity current, while grain-size populations B and C can record different types of flow evolution characterized by the depositional phases of figure 6. Finally, particle-size class D, characterizing the Bouma Tbe sequence, represents the final deposition of a low-density turbidity current.

In addition to these four groups, a fifth group is associated with hybrid or slurry beds (*sensu* Haughton et al., 2009, Muzzi Magalhaes and Tinterri, 2010) deposited by transitional flows (*sensu* Baas et al., 2009, 2011) in which mud dynamics plays a predominant role. These bed types that will be briefly discussed in this work record important phases of decelerations of mud-rich flows controlled especially by particular types of basin morphologies (see Muzzi Magalhaes and Tinterri, 2010; Tinterri et al., 2020 and Tinterri, 2025 for more details). Another very important group of bed types is the contained-reflected beds, which tend to characterize Group D fine-grained facies; these bed types are not discussed in this paper (for more details, see Tinterri et al., 2016, 2022, with references).

Below, the four families or groups of facies, A, B, C, and D, will be discussed.

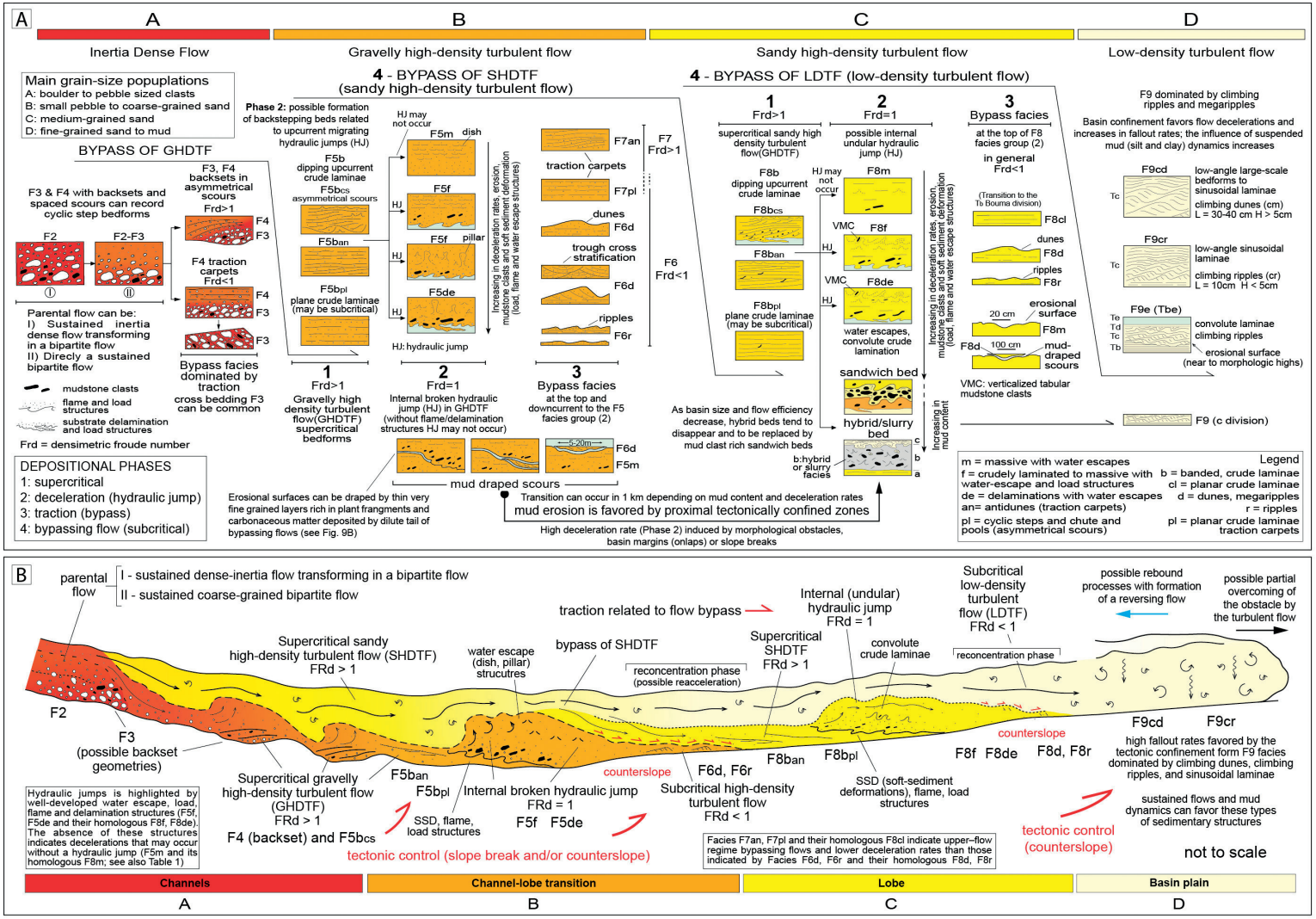

Fig. 6 - A) Predictive turbidite facies-tract scheme based on the interactions between basin morphology and criticality (slightly modified from Tinterri, 2025). This scheme is for turbidite facies deposited in tectonically confined basins characterized by different-scale morphologies. B) Diagram showing the main flow transformations of a bipartite flow during a downslope motion affected by basin confinement and morphological counterslopes. The facies tract is composed of four facies groups (A, B, C, and D) and is characterized by the four depositional phases illustrated in Figure 5, highlighting flow criticality, deceleration, and decoupling processes (see also Table 1). These schemes also try to include the concepts of the previous works (see related sections in the text; see also Mutti et al., 2003, and Postma, 2011). However, it is to be noted that in tectonically confined basins, other types of F9 facies, which are not discussed in this work, can be present. These F9 facies are: a) thin beds above structural highs (Muzzi Magalhaes and Tinterri, 2010), b) ponded and contained-reflected beds (Tinterri et al., 2016, 2022), and c) prodelta deposits (plumites by Mutti, 2019).

Tab. 1 - Summary of facies used in this study (see also Fig. 6). The four main Facies Groups (A, B, C, and D) are consistent with those of Mutti et al. (2003). The depositional phases are consistent with those used in the studies of Hiscott and Middleton (1979), Lowe (1982) and Postma et al. (2009) (see Fig. 5). The legend gives an explanation of the various facies' annotations and their meaning in terms of depositional processes of a fully suspended, decelerating high-density turbidity current (slightly modified from Tinterri, 2025).

<table>
<tr><td colspan="4">Facies Groups based on four dynamic grain–size populations
(see also Figures 1 and 6)</td></tr>
<tr><td>Grain size A
Boulder to pebble sized clasts</td><td>Grain size B
Small pebbles to coarse–grained sand</td><td>Grain size C
Medium–grained sand</td><td>Grain size D
Fine–grained sand to clay</td></tr>
<tr><td>Facies Group A
F2, F3, F4</td><td>Facies Group B
F5, F6, F7</td><td>Facies Group C
F8</td><td>Facies Group D F9</td></tr>
<tr><td colspan="4">Facies resulting from different degrees of deceleration recorded by phases 1-3 (see Figures 5, 6 and 8)</td></tr>
<tr><td>Parental flow transformation</td><td>Depositional phases
1, 2, and 3 in Facies Group B</td><td>Depositional phases
1, 2, and 3 in Facies Group C</td><td>Depositional phase 4</td></tr>
<tr><td rowspan="3">F2, F2-F3
(flow transformations into a sustained bipartite flow)

F3, F4
(traction-bypass and traction carpet phases in a bipartite high-density flow)</td><td>F5bcs, F5ban, F5bpl
(crude lamination-supercritical flow phase 1)</td><td>F8bcs, F8ban, F8bpl
(crude lamination-supercritical flow phase 1)</td><td rowspan="3">F9 (Tbe), F9 cd, F9cr

(subcritical flow phase 4)

(in confined basins, sediment fallout and climbing structures can dominate)</td></tr>
<tr><td>F5m (no hydraulic jump)
F5f, F5de (hydraulic jump)
Hybrid facies
(suspension sedimentation–deceleration phase 2)</td><td>F8m (no hydraulic jump)
F8f, F8de (hydraulic jump)
Hybrid facies
(suspension sedimentation–deceleration phase 2)</td></tr>
<tr><td>F7an, F7pl (upper flow regime) F6d, F6r (lower flow regime) (traction–bypass phase 3)</td><td>F8cl (upper flow regime)
F8d, F8r (lower flow regime)
(traction–bypass phase 3)</td></tr>
</table>

- **b**: banded, spaced or crude lamination (traction-plus-fallout processes in the basal part of a supercritical high–density flow consistent with the traction carpet phase by Lowe, 1982 and Hiscott and Middleton, 1979 – **F5b** and **F8b;** according to the flow velocity, different types of F5b and F8b can occur, i.e., **F5bcs**, **F5ban**, **F5bpl** and **F8bcs**, **F8ban**, **F8bpl**, see Figs. 6,8);
- **m**: crudely laminated to massive facies with water escape structures and devoid of flame structures and substrate delaminations (see below), (**F5m** and **F8m)** characterizing suspension sedimentation without hydraulic jump features (deceleration phase 2; see Figs. 6, 8);
- **f**: facies with load and flame structures (**F5f** and **F8f)** characterizing flow collapse and suspension deposition related to hydraulic jump consistent with the hydraulic jump facies of Postma et al. 2009 and Postma and Cartigny, 2014 (deceleration phase 2; see Figs. 5, 6, 8);
- **de**: substrate delaminations, i.e., local erosional and sand injection features (**F5de** and **F8de)** related to a hydraulic jump but with higher deceleration and fallout rate than those inferred for facies F5f and F8f; load structures can be common (see Fig. 6, 8);
- **Hybrid** or **slurry** facies (*sensu* Haughton et al. 2009 and Muzzi M. and Tinterri, 2010) indicative of flow transformations from mud-rich flows (deceleration phase 2; see Fig. 6);
- **cs:** asymmetrical scours with backsets, cyclic steps and chute and pools (see Figs. 6, 8)
- **an**: undulatory traction carpets and antidunes indicating bypass of an overriding supercritical flow (**F7an**: traction–bypass phase 3)
- **pl and cl**: plane bed traction carpet deposits (**F7pl)** and crude to well-developed plane bed lamination (**F8cl)** indicative of a turbulent flow in the upper–flow regime (traction–bypass phase 3; see Figs. 6, 8);
- **d and r**: dunes (**F6d** and **F8d**) and ripples (**F6r**, **F8r)** recording the bypass of a turbulent flow in the lower–flow regime (traction–bypass phase 3; see Figs. 6, 8);
- **cd and cr**: climbing dunes (**F9cd)** and climbing ripples **(F9cr)** indicative of traction and high fallout rate from a low–density turbulent flow (subcritical phase 4; see Fig. 6, 10).

4.2.1. Facies group A: bipartite parent flow

facies Group A includes paraconglomerates (Facies F2) and orthoconglomerates (Facies F3), (see Mutti et al., 2003). These facies characterize especially channels and/or tectonically controlled conduits, such as for example Fontanelice "channel" in the Marnoso arenacea Formation, northern Apennines (e.g., Ricci Lucchi, 1981; Catto et al., 2024; Tinterri, 2025) or the Ainsa "channel" in the Ainsa basin, south central Pyrenees (see Fig. 7A; see also Cornard and Pickering, 2020).

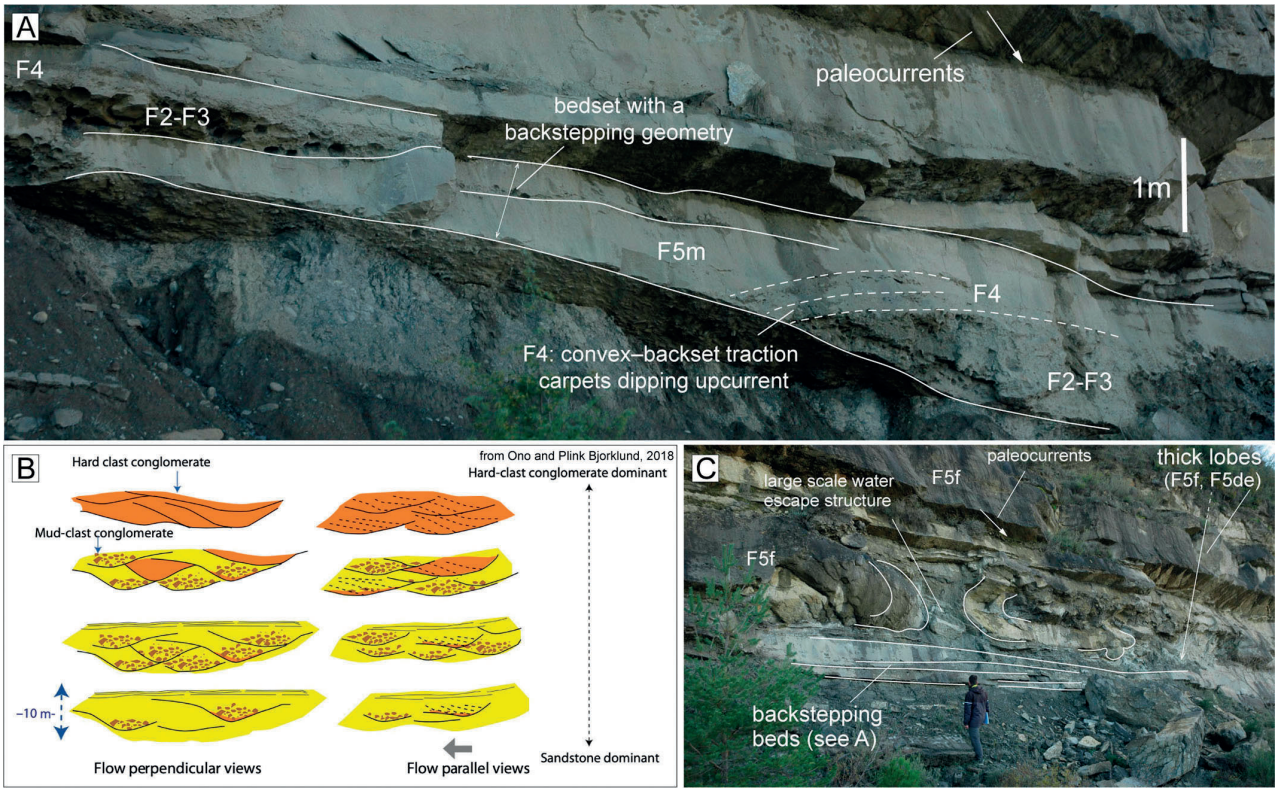

Fig. 7 - Facies of groups A and B. A) lenticular sandy pebble conglomerate (F3, F2–3) rich in mudstone clasts characterized by coarse-grained convex-backset traction carpets (F4) (Ainsa quarry, Eocene, south-central Pyrenees; see also Cornard and Pickering, 2019). B) Submarine-canyon fills interpreted as the deposits of cyclic steps (from Ono and Björklund, 2018). C) Coarse-grained backstepping beds passing upward into thick depositional lobes mainly composed of F5f and F5de characterized by large-scale soft sediment deformations (Ainsa quarry, Eocene, south-central Pyrenees).

According to the type of fluvio-deltaic system and sustained flood-related sediment gravity flows entering seawater, these deposits can be associated with bipartite flows (*sensu* Postma et al., 1988) composed of basal gravelly modified-density grain flows and upper high-density turbulent flow or dense-inertia flows whose transformation (*sensu* Fisher, 1983) can produce a bipartite flow (see also Mutti et al., 2003). The resulting gravelly basal-inertia carpets and related deposits (Facies F3), being deposited by high-velocity sustained flows, may show supercritical bedforms, such as cyclic asymmetrical scours with backsets typical of cyclic steps or chutes and pools (e.g., Lang and Winsemann, 2013; Ono and Plink-Björklund, 2018; Cornard and Pickering, 2020; Englert et al., 2020; Postma et al., 2021; Lang et al., 2021a; Cornard et al., 2025; see also Figs. 6, 7B). Examples of this type of facies can be observed in the tectonically controlled Ainsa basin, well described by Cornard and Pickering (2020) (see Figs. 7A, C).

Facies F3, however, also shows massive facies sometimes reworked in a cross-bedding produced by the traction exerted by the bypass of gravelly high-density flows (Figs. 6, 7A). The transition to the Facies Group B can be characterized by coarse-grained traction carpets (Facies F4), which can show different types of structures, such as convex-backset or plane and parallel geometries, upper flow regime structures (Figs. 6, 7A).

In these settings, an array of asymmetric conglomeratic scour fills, generally exhibiting various types of inclined and laterally accreted crude laminations, may indicate the presence of cyclic steps, thanks also to their similarities with net-erosional cyclic steps found in many modern deep-water canyons and slope systems (e.g., Ono and Plink-Bjorklund, 2018; Lang et al., 2021a; Postma et al., 2016, 2021; Grundvag et al., 2025). It is here believed, however, that our knowledge about the infill of hydraulic-jump-related scours and upper flow regime bedforms in ancient coarse-grained, deep-water slope systems is still relatively limited and enigmatic in many respects (e.g., Massari, 2017; Postma et al., 2021; Grundvag et al., 2025). For this reason, it is considered that more work focusing on this subject would be necessary.

4.2.2. Facies group B: supercritical, deceleration (hydraulic jump) and bypass phases

The deposition of the grain-size population B, due to the transformation of the parental flow induced by a basin topography, gives rise to a bipartite flow characterized by a high-density basal layer dominated by grain-size population B and a fully turbulent upper layer dominated by grain-size populations C and D (Fig. 6 and Tab. 1).

As mentioned above, the facies tract scheme by Tinterri

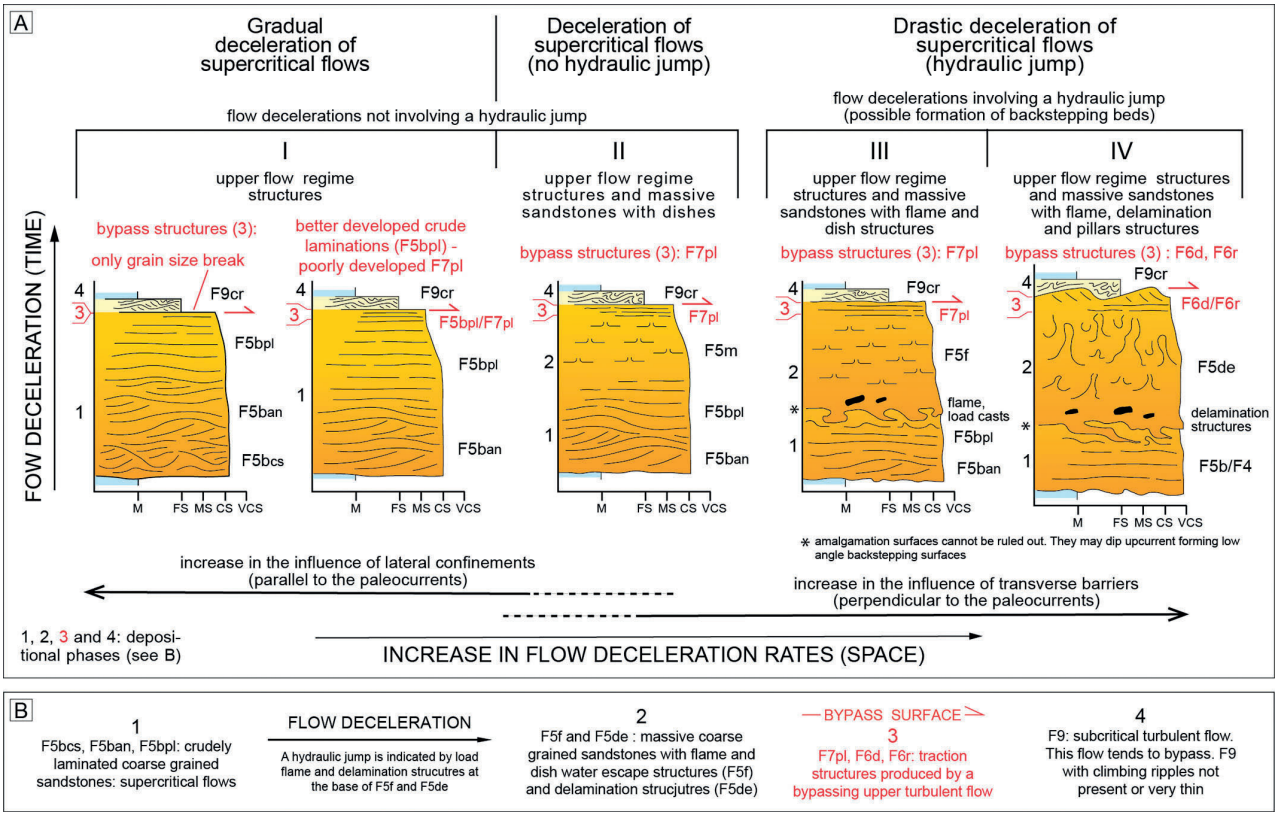

Fig. 8 - Facies sequences characterizing Facies Group B deposited by different rates of flow decelerations that can involve supercritical flows and hydraulic jumps. Their possible relationship with different types of basin configurations is also shown. It is noteworthy that similar facies sequences can also be introduced for the Facies Group C (i.e., facies F8; see text for more details).

(2025) suggests a series of possibilities recording different rates of deceleration of the basal layer that are able to produce different types of facies sequences characterizing Facies Group B (see Fig. 8). These different degrees of flow decelerations, generally induced by various types of basin morphologies, can be highlighted through four main facies sequences that can be observed within the beds (see Fig. 8). These facies sequences are: I) facies F5b entirely composed of crude and spaced laminae in which a vertical passage from supercritical bedforms such as cyclic steps and chute and pools into low angle antidunes and plane and parallel laminae, can be observed; II) Facies F5b passing upward into a Facies F5m (m: massive) characterised by massive sandstones without flame and load structures and with poorly developed water escape structures (dish); III) Facies F5b passing upward abruptly into massive facies characterized by well-developed water escape structures (dish and pillars) and basal flame and load structures (Facies F5f, f: flame, load and water escape structures); IV) Facies F5b passing upward into a massive Facies F5de (de: substrate delaminations and load structures) rich in water escape structures (pillars) whose base is characterized by erosional surfaces and sand injections. In this case, however, amalgamation processes cannot be ruled out.

Beds characterized by these facies sequences can record (from I to IV) a progressive increase in the flow deceleration rates (Fig. 8). In particular, in the first case, Facies F5b, in which asymmetrical scours with upcurrent dipping low-angle cross laminae (cyclic steps and/or chutes and pools) pass upward into low-angle undulatory (antidunes) and plane-parallel lamination, can be interpreted as deposited by supercritical flows characterized by a gradual deceleration. From this point of view, it would also be possible to introduce different categories of F5b according to the characterizing sedimentary structure (see Figs. 6, 8), namely F5bpl (pl: planar crude lamination), F5ban (an: antidunes), and F5bcs (cs: cyclic steps/chute and pools). Conversely, beds composed of facies sequences where F5b passes upward into different types of massive Facies F5, can be interpreted to record a more drastic deceleration and relative collapse of the sediment load transported by the basal dense flow, which may occur through a hydraulic jump or not. More precisely, in the case of a passage from an F5b into an F5m devoid of flame and well-developed water escape structures, flow decelerations should occur without a hydraulic jump (see Section 3, Figs. 6 and 8). Conversely, if the flame and water escape structures are well developed, as in the case of Facies F5f, the deceleration rate, higher than that of the previous case, can form a hydraulic jump (see Section 3, Figs. 6, 7C, 8; see also Postma et al., 2009, Tinterri et al., 2016). The presence of an F5de characterized by delamination and pillar water escape structures would imply even higher deceleration rates with the formation

of well-developed hydraulic jumps. In these two latter cases, upcurrent–migrating hydraulic jumps can form complex backstepping beds composed of multiple scours characterized by alternations of F5b and F5f or F5de (e.g., Postma et al., 2021; Ono et al., 2023; Tinterri, 2025).

These different types of Facies F5, which are well consistent with Facies B1 by Mutti and Ricci Lucchi (1972), record different deceleration degrees of the basal high-density flow, which can be linked to the type of basin, its degree of confinement, and its geometry. For example, beds with facies sequences characterized by Facies F5m and F5f tend to be common in narrowed and confined foredeeps where the deceleration rates begin to be important; conversely, the presence of Facies F5de with erosional bases, delamination structures, and pillar water escape structures is more common in small confined piggyback basins where the deceleration rates are very high. In the same way, beds entirely composed of F5b dominated by supercritical bedforms can be favored by lateral tectonic confinement parallel to the paleocurrents that can act to maintain flow energy and velocity (Figs. 8, 9). Conversely, decelerations able to produce facies F5m, F5f, and F5de can be favored especially by transverse morphologies perpendicular to the paleocurrents that can range from regional tectonic structures (e.g., Tinterri et al., 2020; Piazza et al., 2020) to depositional features such as MTCs and thick depositional lobes (e.g., Tinterri, 2025) (see Figs. 8, 9).

These flow decelerations, induced by basin morphologies, also favor an efficient decoupling process with the deposition of the sediment load transported by the basal high-density flow to form Facies F5b, F5m, F5f, or F5de, and the bypass of the upper turbulent flow, which, exerting efficient traction, can produce well-developed traction structures at the top of the different types of F5 Facies. According to the velocity of the bypassing flow and thus to the deceleration rate, these traction bedforms can range from low-angle-dipping upcurrent (F7an, antidunes) and plane and parallel (F7pl) traction carpets to different types of dunes (F6d) and ripples (F6r) (Figs. 5B, 6A, 8, 9). While the former can be interpreted as related to upper flow regimes, the latter are seen as associated with lower flow regimes, and, consequently, the deceleration rate is higher in the latter case than in the former. Consequently, even the prevalence of one type of bypass structure over the other might be linked to the type of basin and its degree of confinement. For example, the Tortonian deposits of the Marnoso arenacea Formation (northern Apennines, Italy) recording the closure of a large foredeep tend to be dominated by upper–flow–regime bypass structures, i.e., antidunes and plane-parallel traction carpets (F7an and F7pl, Tinterri and Muzzi Magalhaes, 2011; Tinterri, 2025), while particularly narrowed foredeeps or piggyback basins, such as the Annot Sandstones (western Apls, France), and Ranzano Sandstones (northern Apennines), are dominated by subcritical structures, i.e., megaripples and ripples (F6d and F6r; Tinterri et al., 2016, 2017; Tinterri, 2025). In particular, figure 9 shows some bed types coming from the Zumaia Flysch (Eocene, western Pyrenees), where beds dominated by supercritical facies (F5b) in proximal zones pass downcurrent into beds composed of facies sequences recording different degrees of deceleration able to produce hybrid beds and facies F5f overlain by well-developed bypass structures F7pl and F6r (see Fig. 9C). Although a detail facies analysis is still lacking, these facies distributions would suggest a transverse morphology in the Orio and Zarautz area as shown by the stratigraphic studies by Kruitt et al. (1975) and Van Vliet (1982) (see Fig. 9A; see also Pujalte et al., 2000, 2015). In these types of confined basins, indeed, transverse morphologies can produce important decelerations and efficient decoupling phenomena, favouring high-shear stresses exerted by bypassing flows.

Finally, in the F5 facies group, mud-draped scours produced by hydraulic jumps (Mutti and Normark, 1987, 1991) can be common (Fig. 6). Tinterri (2025) stressed that a typical characteristic of the mud-draped scours in these types of settings are erosional surfaces usually draped by thin layers rich in carbonaceous matter and plant fragments. These drapes, deposited by the tail of the bypassing flows (see Fig. 10B), are evidence of extrabasinal sources associated with sustained hyperpycnal flows, which are typical of these basin types (Mutti et al., 2003).

Another type of beds that can characterize Group B facies and that depend on basin morphology are the hybrid-slurry beds (sensu Haughton et al., 2009; Muzzi Magalhaes and Tinterri, 2010). These bed types are generally associated with a well-defined basin conformation that favors the erosion of fine-grained sediment (silt and clay) upcurrent and deceleration in more distal zones of these mud-enriched flows (Muzzi Magalgaes and Tinterri, 2010; Tinterri, 2025). Although these decelerations tend to be favored by structures transverse to paleocurrents in distal zones, hybrid-slurry beds can also characterize more proximal zones of the basin and therefore Group B facies in parts of the basin where deceleration rates are particularly high, such as, for example, against basin margins or structural highs (see Fig. 6A and Tinterri, 2025 for further details).

4.2.3. Facies group C: supercritical, deceleration (hydraulic jump) and bypass phases

After the deceleration phase that provokes the deposition of Group B facies, a reconcentration phase must produce another bipartite flow able to transport the grain size C through the basal high-density layer, while grain-size population D is transported by an upper turbulent, dilute flow (Fig. 6; see also Fig. 1C).

Similarly to the Group B facies, the Group C facies, consisting of medium-grained sand, are produced by various degrees of flow deceleration able to produce beds characterized by facies sequences similar to those of the Group B in which the same depositional phases can be recognized, namely: 1) different types of crudely laminated sandstone deposited by supercritical flows

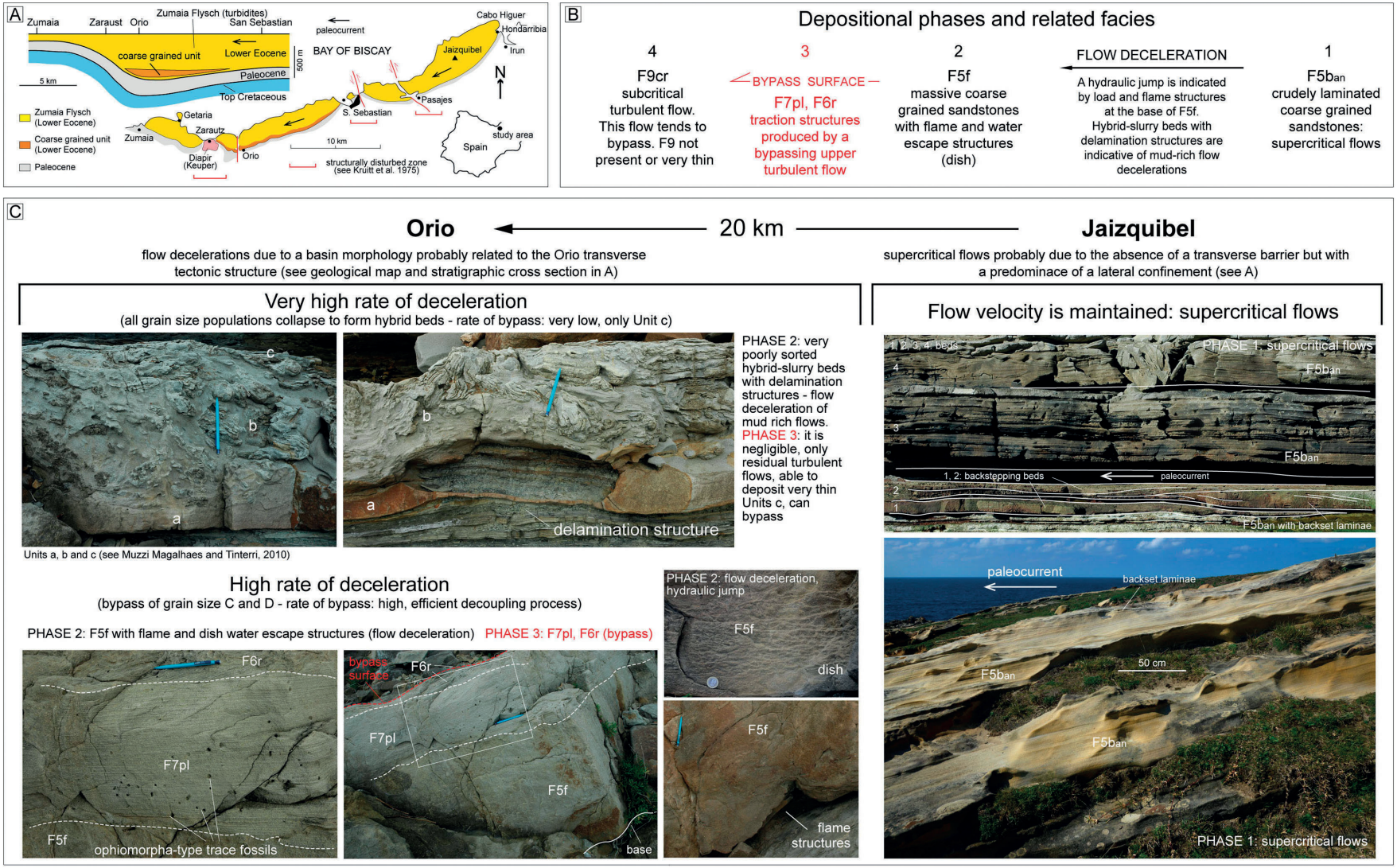

Fig. 9 - Examples of Group B facies deriving from the Zumaia Flysch (Eocene, western Pyrenees). A) Simplified geological map and stratigraphic cross section of the turbidite deposits of the Zumaia Flysch (from Kruitt et al., 1975; Van Vliet, 1982; Pujalte et al., 2000, 2015). B) Explanation of the depositional phases introduced in figure 5 and shown in C. C) Beds dominated by supercritical facies (F5b) in proximal zones (Jaizquibel area) pass downcurrent (Orio area) into beds composed of facies sequences recording different degrees of deceleration able to produce hybrid-slurry beds or facies F5f overlain by well-developed bypass structures F7pl and F6r. This facies distribution is consistent with a transverse structurally disturbed zone characterizing Orio and Zarautz areas, as shown by the stratigraphic data shown in A.

(F8b) — from the lowest to the highest deceleration rate different categories of F8b can occur, i.e., Facies F8bpl (pl: planar crude lamination), F8ban (an: antidunes) and F8bcs (cs: cyclic steps and chute and pools), 2) suspension sedimentation/collapse (possible hydraulic jump) able to deposit three types of massive sandstones with dish structures recording three different degrees of flow deceleration and rate of fallout of the basal high-density flow — from the lowest to the highest deceleration rate, these facies are, Facies F8m (m: massive), F8f (f: flame-load structures) and F8de (de: delamination and load structures), 3) bypass and traction phase able to deposit tractive Facies F8 generated by the bypass of the residual upper low-density flow—from the highest to the lowest bypassing flow velocity, these facies are F8cl (cl: crude plane-parallel laminae), F8d (d: dunes) and F8r (r: ripples). The fourth (4) phase related to the bypassing subcritical flow is recorded by the low-density turbidity current able to transport fine-grained sand and mud (grain-size population D) downcurrent to form Facies F9 (see Fig. 6 and Tab. 1). Group C facies, therefore, represents a more detailed interpretation of facies F8 by Mutti (1992) (i.e., Ta Bouma division) and Facies C by Mutti and Ricci Lucchi (1972).

As in the case of Group B, the facies of Group C can form sequences that record varying degrees of flow deceleration, again indicative of different basin morphologies. For example, the predominance of beds composed of F8b entirely composed of different types of crude lamination can be interpreted as deposited by gradually decelerating supercritical flows, favored, more likely, by lateral tectonic confinements (i.e., parallel to the paleocurrents) that act by conserving the energy and velocity of the flows. Conversely, beds characterized by facies sequences in which Facies F8b pass upward into different types of massive sandstones can be interpreted as recording a relatively high degree of deceleration of the basal high-density flow, which can be particularly favored by morphological barriers transverse to the paleocurrents. These decelerations can occur without a hydraulic jump if flame and load structures are not present (see Facies F8m) or may be marked by a hydraulic jump when these structures, together with water escape dish structures, are well developed (see Facies F8f and F8de). In particular, Facies F8de, with erosional and delamination structures, can be interpreted to represent the facies recording the highest rate of deceleration. In these cases, upcurrent-migrating hydraulic jumps, whose energy, however, should be less than that characterizing Group B facies, may form complex backstepping beds. In the same way, although perhaps slightly less evident than the similar facies of Group B, mud-draped scours related to hydraulic jumps can also be common in Facies Group C. They are more evident especially in situations that favor deceleration and decoupling processes, such as tectonically confined basins or at the top of depositional lobes, whose morphology, creating an adverse slope to the flow, can induce significant decelerations and choking of the flows (i.e., a hydraulic jump; Tinterri, 2025). As mentioned above, it is here stressed that density stratification of the flows can play an important role in the required height of the obstruction to produce a hydraulic jump, i.e., dilute flows with high velocities require a very large stepped obstruction, many times larger than the flow thickness, to trigger a jump, while high-density flows with relatively low velocities require very small steps (see Fig. 4A, Hamilton et al., 2015; Postma et al., 2016; Scacchia et al., 2022b; Englert et al., 2024; Tinterri, 2025).

Finally, the deceleration-hydraulic jump phase induced by different types of basin morphologies favors a second decoupling process, which, producing an efficient bypass of upper dilute low-density flow (bypass phase 3), can form bypass structures at the top of the massive Facies F8m, F8f, and F8de. These traction structures range from crude to well-developed plane and parallel lamination (F8cl) up to dunes and ripples (F8d and F8r, respectively) and can be interpreted as upper- to lower-flow-regime bedforms, respectively. The tractive structures (perfectly homologous to the coarser Facies F6 and F7 characterizing facies group B) record the passage into facies F9 (i.e., Bouma Tbe divisions) deposited by the bypassed low-density turbidity current able to transport the residual grain-size population D more downcurrent (see Figs. 6B, 10).

4.2.4. Facies group D: deceleration of a low-density turbulent flow (f9 dominated by climbing dunes and ripples)

The facies tract scheme by Tinterri (2025) gives a particular interpretation of the F9 facies deposited in tectonically controlled confined basins by residual bypassing low-density flows (depositional phase 4; see Fig. 10A). In these settings, indeed, Facies F9 are always dominated by well-developed climbing bedforms, such as climbing dunes, climbing ripples, and low-angle wavy to sinusoidal structures (Figs. 10 B,C,D). The widespread presence of these types of traction-plus-fallout structures (generally uncommon in less confined basins) is interpreted as an interaction between dynamics of very fine-grained sediment (e.g., Baker and Baas, 2020; Baas et al., 2021; Taylor et al., 2024) and an increase in fallout rates (e.g., suspension/traction ratio) favored by the deceleration of low-density turbulent flows (e.g., Jopling and Walker, 1968; Jobe et al., 2012). Tinterri (2025) suggests that these depletive flows are favored by regional subtle slope breaks or counterslopes, which, in these basin types, are generally associated with important transversal tectonic structures (Fig. 10A). These morphological elements, indeed, may induce gradual and progressive decelerations favoring fallout-rate increases and thus climbing structures (Fig. 10). Therefore, the interpretation by Tinterri (2025) of F9 facies is particularly interesting because, if accurate, the occurrence of climbing structures, in addition to being

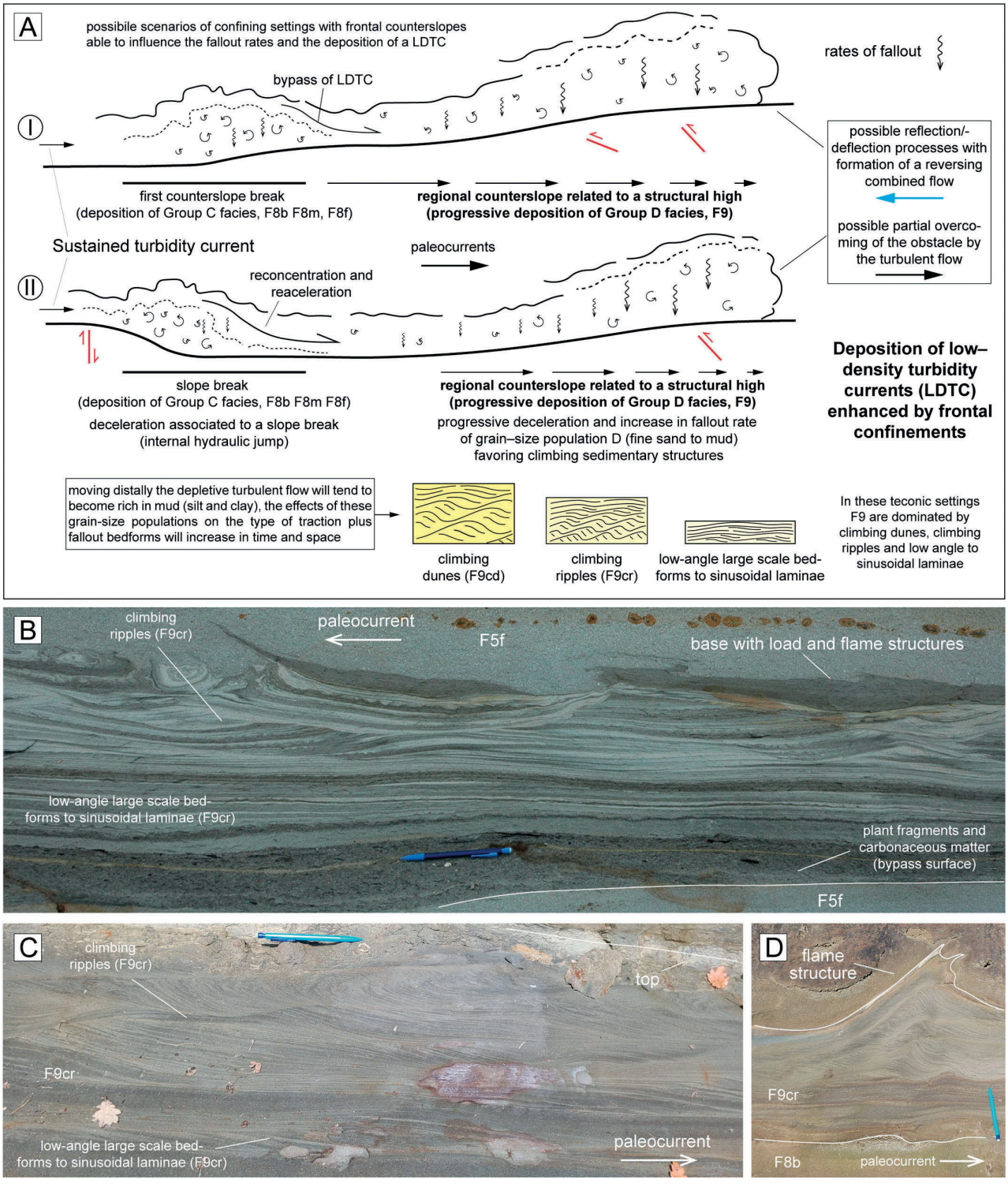

Fig. 10 - A) Model to explain climbing ripples, climbing dunes, low-angle climbing megaripples, and sinusoidal laminae as related to the increase in the fallout rate and traction-plus-fallout processes due to the progressive deceleration of low-density turbidity currents induced by basin morphologies, such as slope breaks and counterslopes (from Tinterri, 2025). Dynamics of silt and clay in sustained, long-lived turbidity currents may further favor these types of structures. B, C and D) Examples of well-developed climbing structures in tectonically confined basins; B is from Maceiò Formation (Cretaceous, Brazil), while C and D are from Fontanelice–Sarsina turbidite system in the Fontanelice area (Miocene, Marnoso arenacea Formation, northern Apennines). It is to be noted that flame and load structures are indicative of rapid depositions related to flow decelerations.

favored by sustained turbidity currents triggered by hyperpycnal flows (e.g., Mutti et al., 2003), can also be linked to particular basin conformations and thus be diagnostic not only of the type of basin but also of its morphologic characteristics.

5. DISCUSSION AND CONCLUSIONS

The facies scheme in figure 6 (see also Tab. 1), characterized by four facies groups consistent with the four dynamic grain-size populations A, B, C, and D, records the deceleration of a bipartite flow that gradually transforms and becomes finer grained downcurrent. These flow transformations, enhanced by regional counterslopes generally associated with transverse synsedimentary tectonic structures, occur through three efficient decoupling processes, namely: 1) the bypass of a gravelly high-density flow (grain-size population B) on a dense conglomeratic basal flow (a sort of modified density basal grain flow *sensu* Lowe 1976) able to deposit the Group A facies; 2) the bypass of a sandy high-density turbidity current (grain-size population C) on a dense gravel basal flow able to deposit the Group B facies; and 3) the bypass of a low-density turbulent dilute flow (grain–size population D) on a dense sandy basal flow able to deposit the Group C facies. The deceleration phases can produce different types of facies sequences (Fig. 8) characterized by the four depositional phases shown in figures 5 and 6. Conversely, the decelerations of low-density turbidity currents, also favored by the confinement of the basin, are characterized by a downcurrent increase in well-developed climbing ripples and dunes produced by progressive increase in fallout rates in fine-grained sediments, in which the occurrence of silt and clay can further favor the formation of these types of structures (Fig. 10).

The new facies scheme, in conclusion, can be considered diagnostic of situations that favor deceleration and decoupling processes, such as basins in which the tectonics act to create a confined setting (i.e., narrowed foredeeps and wedge-top basins). In these settings, slurry-hybrid and contained-reflected beds are two other types of beds fundamental for understanding turbidite deposition influenced by tectonically controlled basin morphologies and geometries (see Fig. 6). The facies scheme, indeed, also takes into account hybrid event beds in various basin settings, i.e., a category of bed types whose formation is strongly linked to the morphology and degree of confinement of the basin, as highlighted by Muzzi Magalhaes and Tinterri (2010), Tinterri et al. (2020) and Tinterri (2025, see his Fig. 17).

Of consequence, the work by Tinterri (2025) shows that the degree of tectonic confinement can modify the flow's efficiency (i.e., the ability of the flow to transform, evolve, and segregate grain-size populations in distinct facies; see Mutti, 1979; Mutti et al., 1999). This is particularly evident in turbidite systems located in narrowed foredeep and wedge-top basins where different types of morphologies confine, laterally and frontally, turbidity currents. At large scales, basin morphologies are generally associated with regional transversal structural alignments, while, at smaller scales, they can be related to depositional features, such as MTCs and depositional lobes, which can become very thick in confined basin settings (Fig. 4A). Whilst lateral tectonic confinement favors conservation of flow energy and thus supercritical flows, transversal structures are features that can control flow deceleration, transformation, reflection, and, thus, sediment deposition or bypass and, ultimately, flow efficiency (see Figs. 6, 8, 9). Consequently, flow efficiency should have a broader meaning than that given by Mutti et al. (1999) (see also Mutti, 1979, 1985) and is thus the sum of: 1) the type of flow and its capacity to transform, 2) the type of basin and its size, and 3) the basin physiography. The latter two parameters control how a flow will transform and thus how drastic modification can occur in the classic facies tracts produced by waning and depletive flows. This is clearly shown by the works on the foredeep turbidites of Marnoso-arenacea and Cervarola Sandstone formations (northern Apennines, Italy) where every tectonically controlled stratigraphic unit is characterized by a well-determined facies tract (see Tinterri and Muzzi Magalhaes, 2011; Tinterri and Piazza, 2019). Thus, a basin modification due to the tectonics is always associated with a concomitant modification in the type of facies tract and in the vertical and lateral facies distribution (Figs. 6, 8, 9; see also Muzzi Magalhaes and Tinterri, 2010; Tinterri and Piazza, 2019). Although various works give particular emphasis to the type of feeder system and thus turbidity–current triggering mechanisms on the type of resulting facies tract (e.g., Mutti et al., 2003; Zavala and Arcuri, 2021), this work, while recognizing the importance of the feeder system type (e.g., Tinterri et al., 2020), emphasizes the key role of the tectonically controlled basin morphology on the flow processes, highlighting how the basin shape, favoring or hindering flow evolution, can control the facies–tract type, which, in turn, may become diagnostic of a well-determined basin type and physiography and *vice versa.*

ACKNOWLEDGEMENTS - The author is grateful to Emiliano Mutti for his teachings and discussions over the years on turbidites and beyond, and to many other people with whom he has discussed many problems concerning foreland sedimentation and, particularly, Pierre Muzzi Magalhaes, Bruno Catto, Rogerio Soares Cunha, and Fabrizio Lima (Petrobras) Giancarlo Davoli, Alessio Tagliaferri, Andrea Civa and Marco Fonnesu (ENI), and Salvatore Milli, Alberto Piazza, Michele Laporta, Vanni Pizzati, Elena Scacchia and Simone Lombardi. The author also thanks George Postma, David Hoyal, Timothy Demko, Juan Fedele (ExxonMobil), and Fabiano Gamberi for the discussions on supercritical-flow deposits. The author is also deeply grateful to Salvatore Milli for his helpful and constructive comments. A large part of this research was generously funded by ENI, Petrobras, and ExxonMobil.

REFERENCES

Alexander J., Bridge J.S., Cheel R.J., Leclair S.F., 2001. Bedforms and associated sedimentary structures formed under water flows over aggrading sand beds. Sedimentology 48, 133-152.

Amy L.A., McCaffrey W.D., Kneller B.C., 2004. The influence of a lateral basin-slope on the depositional patterns of natural of experimental turbidity currents. In: Joseph P., Lomas S.A. (Eds.), Deep-water Sedimentation in the Alpine Foreland Basin of the SE Francia: New Perspectives on the Grès d'Annot and Related Systems. Geological Society Special Publication 221, 311-330.

Amy L.A., Kneller B.C., McCaffrey W.D., 2007. Facies architecture of the Gres de Peïra Cava, SE France: landward stacking patterns in ponded turbiditic basins. Journal of the Geological Society of London 164, 143-162.

Baas J.H., Best J.L., Peakall J., Wang M., 2009. A phase diagram for turbulent, transitional, and laminar clay suspension flows. Journal of Sedimentary Research 79, 162-183.

Baas J.H., Best J.L., Peakall J., 2011. Depositional processes, bedform development and hybrid bed formation in rapidly decelerated cohesive (mud-sand) sediment flows. Sedimentology 58, 1953-1987.

Baas J.H., Best J., Peakall J., 2021. Rapid gravity flow transformation revealed in a single climbing ripple. Geology 49, 493-497.

Baker M.L., Baas J.H., 2020. Mixed sand-mud bedforms produced by transient turbulent flows in the fringe of submarine fans: indicators of flow transformation. Sedimentology 67, 2645-2671.

Bouma A., 1962. Sedimentology of some flysch deposits, a graphic approach to facies interpretation. Elsevier, Amsterdam, pp. 168.

Bridge J.S., 2003. Rivers and Floodplains; Forms, Processes and Sedimentary Record. Blackwell, Oxford, pp. 491.

Campbell C.V., 1967. Lamina, laminaset, bed, and bedset. Sedimentology 8, 7-26.

Cartigny M.J.B., Postma G., 2016. Turbidity current bedforms. In: Guillén J., Acosta J., Palanques A., Chiocci F.L. (Eds.), Atlas of Bedforms in the Western Mediterranean. Springer, Heidelberg, 1-5.

Cartigny M.J.B., Postma G., van den Berg J.H., Matsbergen D.R., 2011. A comparative study of sediment waves and cyclic steps based on geometries, internal structures and numerical modelling. Marine Geology 280, 40-56.

Cartigny M.J.B., Eggenhuisen J.T., Hansen E.W.M., Postma G., 2013. Concentration dependent flow stratification in experimental high-density turbidity currents and their relevance to turbidite facies models. Journal of Sedimentary Research 83, 1046-1064.

Cartigny M.J.B., Ventra D., Postma G., Van Den Berg J.H., 2014. Morphodynamics and sedimentary structures of bedforms under supercritical-flow conditions: new insights from flume experiments. Sedimentology 61, 712-748.

Catto B., Muzzi Magalhaes P., Tinterri R., 2024. Control of the synsedimentary tectonics on turbidite channels dynamics: an integrated study between field and subsurface data. Società Geologica Italiana (SGI) and Società Italiana di Mineralogia e Petrologia (SIMP) Joint Congress, Bari 3-5 September 2024, Abstract book, 1095.

Cornard P.H., Pickering K.T., 2019. Supercritical-flow deposits and their distribution in a submarine channel system, middle Eocene, Ainsa Basin, Spanish Pyrenees. Journal of Sedimentary Research 89, 576–597.

Cornard P.H., Pickering K.T., 2020. Submarine topographic control on distribution in supercritical-flow deposits in lobe and related environments, middle Eocene, Jaca basin, Spanish Pyrenees. Journal of Sedimentary Research 90, 1222-1243.

Cornard P.H., Pickering K.T., Strasser M., 2025. Supercritical-flow deposits: a new quantitative tool to characterise deep-marine depositional environments (Oligocene Annot Sandstones, SE France). Terra Nova 34, 49-56.

Cunha R.S., Tinterri R., Muzzi Magalhaes P., 2017. Annot Sandstone in the Peïra Cava basin: An example of an asymmetric facies distribution in a confined turbidite system (SE France). Marine and Petroleum Geology 87, 60-79.

Demko T., Fedele J.J., Hoyal D.C., Pederson K., Hamilton P., Abreu V., Postma G., 2014. Bedforms indicative of supercritical flow in steep, sandy submarine fans and fan deltas: Ainsa, Ebro and Tabernas Basins, Spain. In: Geological Society of America, Annual Meeting, Vancouver, 19-22 October 2014, Abstract Book, Paper no. 345-5.

Dorrell E.M., Peakall J., Sumner E.J., Parsons D.R., Darby S.E., Wynn R.B., Özsoy E., Tezcan D., 2016. Flow dynamics and mixing processes in hydraulic jump arrays: Implications for channel–lobe transition zones. Marine Geology 381, 181-193.

Englert R.G., Hubbard S.M., Cartigny M.J.B., Clare M.A., Coutts D.S., Hage S., Clarke J.H., Jobe Z., Linter D.G., Stacey C., Vendettuoli D., 2020. Quantifying the three-dimensional stratigraphic expression of cyclic steps by integrating seafloor and deep-water outcrop observations. Sedimentology 69, 1465-1501.

Englert R.G., Hubbard S.M., Romans B., Kaempfe S., Bell D., Nesbit P.R. Stright L., 2024. Flow dynamics as Froude-supercritical turbidity currents encounter metre-scale slope minibasin topography. The Depositional Record 10, 527-558.

Fedele J.J., Hoyal D., Barnaal Z., Tulenko J., Awalt S., 2016. Bedform created by gravity flows. In: Budd D.A., Hajek E.A., Purkis S.J. (Eds.), Autogenic Dynamics and Self-Organization in Sedimentary Systems. SEPM, Special Publication 106, 95-121.

Fielding C.R., 2006. Upper flow regime sheets, lenses and scour fills: extending the range of architectural elements for fluvial sediments bodies. Sedimentary Geology 190, 227-240.

Fisher R.V., 1983. Flow transformation in sediment gravity flows. Geology 11, 273-274.

Fricke A.T., Sheets B.A., Nittrouer C.A., Allison M.A., Ogston A.S., 2015. An examination of Froude-supercritical flows and cyclic steps on a subaqueous lacustrine delta, Lake Chela, Washington, U.S.A.. Journal of Sedimentary Research 85, 754-767.

Gallicchio S., Cerone D., Tinterri R., 2023. Depositional record of confined turbidites in synsubduction intraslope basin: insight from the Tufiti di Tusa Formation (Southern Apennines, Italy). Marine and Petroleum Geology 147, 105969.

Garcia M.H., 1993. Hydraulic jumps in sediment-driven bottom currents. Journal of Hydraulic Engineering 119, 1094-1117.

Garcia M.H., Parker G., 1989. Experiments on hydraulic jumps in turbidity currents near a canyon-fan transition. Science 117, 393-396.

Gray T.E., Alexander J., Leeder M.R., 2005. Quantifying velocity and turbulence structure in depositing sustained turbidity currents across breaks in slope. Sedimentology 52, 467-488.

Grundvag S.A., Henstra G.A., Rotevatn A., Salomon E., Kristensen T.B. 2025. Signatures of hydraulic jump-related scouring in a deep-marine rift basin, Wollaston Forland Group, NE Greenland. Sedimentary Geology 487, 106944.

Hage S., Cartigny M.J.B., Clare M.A., Sumner E.J., Vendettuoli D., Hughes Clarke J.E., Hubbard S.M., Talling P.J., Lintern D.G., Stacey C.D., Englert R.G., Vardy M.E., Hunt J.E., Yokokawa M., Parsons D.R., Hizzett J.L., Azpiroz-Zabala M., Vellinga A.J., 2018. How to recognize crescentic bedforms by supercritical turbidity currents in the geologic record: insight from active submarine channels. Geology 46, 563-566.

Hamilton P.B., Strom K.B., Hoyal D.C., 2015. Hydraulic and sediment transport properties of autogenic avulsion cycles on submarine fans with supercritical distributaries. Journal of Geophysical Research, Earth Surface 120, 1369-1389

Hamilton P.B., Gaillot G., Strom K., Fedele J.J., Hoyal D., 2017. Linking hydraulic properties in supercritical submarine distributary channel to depositional-lobe geometry. Journal of Sedimentary Research 87, 935-950.

Hand B.M., 1974. Supercritical flow in density currents. Journal of Sedimentary Petrology 44, 637-648.

Harms J.C., Fahnestock P., 1965. Stratification, bed forms and flow phenomena (with an example form Rio Grande). In: Middleton G.V. (Ed.), Primary Sedimentary Structures and Their Hydrodynamic Interpretation. SEPM, Special Publication 12, 84-115.

Haughton P.D.W., Davis C., Mcaffrey W., Barker S.P., 2009. Hybrid sediment gravity flow deposits-classification, origin and significance. Marine and Petroleum Geology 26, 1900-1918.

Henstra G.A., Grundvåg S.-A., Johannessen E.P., Kristensen T.B., Midtkandal I., Nystuen J.P., Rotevatn A., Surlyk F., Sæther T., Windelstad J., 2016. Depositional processes and stratigraphic architecture within a coarse-grained rift-margin turbidite system: the Wollaston Forland Group, East Greenland. Marine and Petroleum Geology 76, 187-209.

Hiscott R.N., 1994. Loss of capacity, not competence, as the fundamental process governing deposition from turbidity currents. Journal of Sedimentary Research A64, 209-214.

Hiscott R.N., Middleton G.V., 1979. Fabric of coarse deep-water sandstones, Tourelle Formation, Quebec, Canada. Journal of Sedimentary Petrology 50, 703-721.

Hodgson D.M., Peakall J., Maier K.L., 2022. Submarine channel mouth settings: processes, geomorpholgy and feposits. Frontiers of Earth Science 10, 790320.

Hofstra M., Hodgson D., Peakall J., Flint S., 2015. Giant scour-fills in ancient channel- lobe transition zones: formative processes and depositional architecture. Sedimentary Geology 329, 98-114.

Hoyal D.C., Demko T., Postma G., Wellner R.W., Pederson K., Abreu V., Fedele J.J., Box D., Sprague A., Kaveh G., Strom K., Hamilton P., 2014. Evolution, architecture and stratigraphy of Froude supercritical submarine fans. American Association of Petroleum Geologists, Search and Discovery, Article 90189.

Howlett D.M, Ge Z., Nemec W., Gawthorpe R.L., Rotevatn A., Jackson C.A.L., 2019. Response of unconfined turbidity current to deep-water fold and thrust belt topography: Orthogonal incidence on solitary and segmented folds. Sedimentology 66, 2425-2454.

Jobe Z., Lowe D.R., Morris W.R., 2012. Climbing-ripple successions in turbidite systems: depositional environments, sedimentation rates and accumulation times. Sedimentology 59, 867-898.

Jopling A.V., Richardson E.V., 1966. Backset bedding developed in shooting flow in laboratory experiments. Journal of Sedimentary Petrology 36, 821-825.

Jopling A.V., Walker R.G., 1968. Morphology and origin of ripple-drift cross-lamination, with examples from the Pleistocene of Massachusetts. Journal of Sedimentary Petrology 38, 971-984.

Kneller B.C., McCaffrey W.D., 1999. Depositional effects of flow nonuniformity and stratification within turbidity currents approaching a bounding slope: deflection, reflection, and facies variation. Journal of Sedimentary Research 69, 980-991.

Kneller B.C., McCaffrey W.D., 2003. The interpretation of vertical sequences in turbidite beds: the influence of longitudinal flow structure. Journal of Sedimentary Research 73, 706-713.

Komar P.D., 1971. Hydraulic jumps in turbidity currents. Geological Society of America Bulletin 82, 1477-1488.

Kostic S., 2011. Modelling of submarine cyclic steps: controls on their formations, migrations and architecture. Geosphere 7, 294-304.

Kostic S., Parker G., 2006. The response of turbidity currents to a canyon-fan transition: internal hydraulic jumps and depositional signatures. Journal of Hydraulic Research 44, 631-653.

Kruit C., Brouwer J., Knox G., Schollnberger W. Van Vliet A., 1975. Une excursion aux cones d'alluvions en eau profonde d'age Tertiare pres de San Sebastian (Province de Guipuzcoa, Espagne. In: Guide Excursion Z-23, 9th Congress International of Sedimentologists, Nice, pp. 75.

Ito M., Ishikawa K., Nishida N., 2014. Distinctive erosional and depositional structures formed at a canyon mouth: a lower Pleistocene deep-water succession in the Kasuza forearc basin on the Boso Peninsula, Japan. Sedimentology 61, 2042-2062.

Lang J., Winsemann J., 2013. Lateral and vertical facies relationship of bedforms deposited by aggrading supercritical flows: from cyclic steps to humpback dunes.

Sedimentary Geology 296, 36-54.

Lang J., Brandes C., Winsemann J., 2017. Erosion and deposition by supercritical flows during channel avulsion and backfilling: field examples from coarse-grained deepwater channel-levee complexes (Sandino Forearc Basin, Southern Central America). Sedimentary Geology 349, 79-102.

Lang J., Le Heron D.P., Van den Berg J.H., Winsemann J., 2021a. Bedforms and sedimentary structures related to supercritical flows in glacigenic settings. Sedimentology 68, 1539-1579.

Lang J., Fedele J.J., Hoyal D.C.J.D., 2021b. Three-dimensional submerged wall jets and their transition to density flows. Morphodynamics and implications for the depositional record. Sedimentology 68, 1297-1327.

Lowe D.R., 1976. Grain flow and grain flow deposits. Journal of Sedimentary Petrology 46, 188-199.

Lowe D.R., 1982. Sediment gravity flows: depositional models with special reference to the deposits of high-density turbidity currents. Journal of Sedimentary Petrology 52, 279-297.

Lowe D.R., 1988. Suspended-load fallout rate as an independent variable in the analysis of current structures. Sedimentology 35, 921-929.

Massari, F., 1984. Resedimented Conglomerates of a Miocene Fan-Delta Complex, Southern Alps, Italy. In: Koster E.H., Steel R.J. (Eds.), Sedimentology of Gravels and Conglomerates. Canadian Society of Petroleum Geologists, Memoir 10, 259-278.

Massari F. 2017. Supercritical-flow structures (backset-bedded sets and sediment waves) on high-gradient clinoform systems influenced by shallow-marine hydrodynamics. Sedimentary Geology 360, 73-95.

Menard H.W., 1964. Marine Geology of the Pacific. McGraw-Hill, New York., pp. 271.

Middleton G.V., 1965. Antidune cross bedding in a large flume. Journal of Sedimentary Petrology 35, 922-927.

Middleton G.V., 1966. Experiments on density turbidity currents. II. Uniform flow of density currents. Canadian Journal of Earth Sciences 3, 627-637.

Mutti E., 1979. Turbidites et cônes sous-marins profonds. In: Homewood P. (Ed.), Sédimentation Détritique. Institut de Géologie, Université de Fribourg, Fribourg, 353-419.

Mutti E., 1985. Turbidite systems and their relations to depositional sequences. In: Zuffa G.G., (Ed.), Provenance of Arenites. NATO-ASI Series, Reidel Publishing Co., 65-93.

Mutti E., 1992. Turbidite Sandstones. Agip, Istituto di Geologia, Università di Parma, San Donato Milanese, pp. 275.

Mutti E., 2019. Thin-bedded plumites: an overlooked deep-water deposit. Journal of Mediterranean Earth Sciences 11, 61-80.

Mutti E., 2023. Turbidite Systems: Outcrop-Based Analysis. Petrobras book publication, pp. 466.

Mutti E., Normark W.R., 1987. Comparing examples of modern and ancient turbidite systems: problems and concepts. In: Leggett J.K., Zuffa G.G. (Eds.), Marine Clastic Sedimentology, London, Graham and Trotman, 1-38.

Mutti E., Normark W.R., 1991. An integrated approach to the study of turbidite systems. In: Weimer P., Link M.H. (Eds.), Seismic Facies and Sedimentary Processes of Submarine Fans and Turbidite Systems. Springer-Verlag, New York, 75-106.

Mutti E., Ricci Lucchi F., 1972. Le torbiditi dell'Appennino Settentrionale: introduzione all'analisi di facies. Memorie della Società Geologica Italiana 11, 161-199.

Mutti E., Tinterri R., Remacha E., Mavilla N., Angella S., Fava L., 1999. An introduction to the analysis of ancient turbidite basins from an outcrop perspective. American Association of Petroleum Geologists, Continuing Education Course Note Series 39, pp. 93.

Mutti E., Tinterri R., Benevelli G., Di Biase D., Cavanna G., 2003. Deltaic, mixed and turbidite sedimentation of ancient foreland basins. Marine and Petroleum Geology 20, 733-755.

Mutti E., Bernoulli D., Ricci Lucchi F., Tinterri R., 2009. Turbidites and turbidity currents from Alpine "flysch" to the exploration of continental margins. Sedimentology 56, 267-318.

Muzzi Magalhaes P., Tinterri R., 2010. Stratigraphy and depositional setting of slurry and contained (reflected) beds in the Marnoso-arenacea Formation (Langhian-Serravallian) Northern Apennines, Italy. Sedimentology 57, 1685-1720.

Ono K., Plink-Björklund P., 2018. Froude supercritical flow bedforms in deepwater slope channel? Field examples in conglomerates, sandstones and fine-grained deposits. Sedimentology 65, 639-669.

Ono K., Plink-Björklund P., Eggenhuisen J.T., Matthieu J.B., Cartigny M.J.B., 2021. Froude supercritical flow processes and sedimentary structures: New insights from experiments with a wide range of grain sizes. Sedimentology 68, 1328-1357.

Ono K., Naruse H., Yao Q., Cai Z., Fokuda S., Yokokawa M., 2023. Multiple scours and upward fining caused by hydraulic jumps: implications for the recognition of cyclic steps in the deepwater stratigraphic record. Journal of Sedimentary Research 93, 243-255.

Piazza A., Tinterri R., 2019. The foredeep turbidites of the Macigno Sandstones Formation (Chattian–Aquitanian, northern Apennines, Italy). 34th International Meeting of the International Association of Sedimentologists, Rome 10-13 September 2019, Abstract Book, p. 1570.

Piazza A., Tinterri R., 2020. Cyclic stacking pattern, architecture and facies of the turbidite lobes in the Macigno sandstones formation (Chattian–Aquitanian, northern Apennines, Italy). Marine and Petroleum Geology 122, 104704.

Piazza A., Tinterri R., Artoni A., 2020. The role of orogen-transversal tectonic structures on the "syn"and "post" depositional evolution of a foredeep succession: The case of the Cervarola Sandstones Formation, Miocene, Northern Apennines, Italy. Tectonophysics 778, 228367.

Pickering K.T., Hiscott R.N., 1985. Contained (reflected) turbidity currents from the Middle Ordovician Cloridorme Formation, Quebec, Canada: an alternative to the antidune hypothesis. Sedimentology 32, 373-394.

Pickering K.T., Hiscott R.N., 2016. Deep Marine Systems: Processes, Deposits, Environments, Tectonics and

Sedimentation. Wiley, Oxford, pp. 657.

Piper D.J.W., Normark W.R., 2001. Sandy fans form Amazon to Hueneme and beyond. American Association of Petroleum Geologists Bulletin 85, 1407-1438.

Pizzati V., Tinterri R., 2023. The influence of confining morphology on lateral and vertical turbidite facies distribution (Firenzuola turbidite system, Marnoso-arenacea Formation, Italy). 36th International Meeting of the International Association of Sedimentologists, Poster Contribution, Abstract book, p. 265.

Pohl F., Eggenhuisen J.T., Tilston M., Cartigny M.J.B., 2019. New flow relaxation mechanism explains scour fields at the end of submarine channels. Nature Communications 10, 4425.

Pohl F., Eggenhuisen J.T., Cartigny M.J.B., Tilston M.C., De Leeuw J., Hermidas N., 2020. The influence of a slope break on turbidite deposits: an experimental investigation. Marine Geology 424, 106160.

Pohl F., Eggenhuisen J.T., Cartigny M.J.B., Tilston M.C., 2022. Initiation of deposition in supercritical turbidity currents downstream of a slope break. EarthArXiv.

Postma G., 2011. Sediment gravity flow. In: Singh V.P., Singh P., Haritashya U.K. (Eds.), Encyclopedia of Snow, Ice and Glaciers: Springer, 1005-1010.

Postma G, Cartigny M.J.B., 2014. Super and subcritical turbidity currents and their deposits—a synthesis. Geology 42, 987-990.

Postma G., Kleverlaan K., 2018. Supercritical flows and their control on the architecture and facies of small-radius sand-rich fan lobes. Sedimentary Geology 364, 53-70.

Postma G., Nemec W., Kleinsphen K.L., 1988. Large floating clasts in turbidites: a mechanism for their emplacement. Sedimentary Geology 58, 47-61.

Postma G., Cartigny M.J.B., Kleverlaan K., 2009. Structureless, coarse-tail graded Bouma Ta formed by internal hydraulic jump of the turbidity-current. Sedimentary Geology 219, 1-6.

Postma G., Kleverlaan K., Cartigny M.J.B, 2014. Recognition of cyclic steps in sandy and gravelly turbidite sequences and consequences for the Bouma facies model. Sedimentology 61, 2268-2290.

Postma G., Hoyal D.C., Abreu V., Cartigny M.J.B., Demko T., Fedele J.J., Kleverlaan K., Pederson K.H., 2016. Morphodynamics of supercritical turbidity currents in the channel-lobe transition zone. In: Lamarche G., Mountjoy J., Bull S., Hubble T., Krastel S., Lane E., Micallef A., Moscardelli L., Mueller C., Pecher I., (Eds.), Submarine Mass Movements and Their Consequences, Advances in Natural and Technological Hazard Research. Springer 47, 469-478.

Postma G., Lang J., Hoyal D.C., Fedele J.J., Demko T., Abreu V., Pederson K.H., 2021. Reconstruction of bedforms dynamics controlled by supercritical flow in the channel–lobe transition zone of a deep–water delta (Sant Llorenç del Munt, north-east Spain, Eocene). Sedimentology 68, 1674-1697.

Pujalte V., Robles S., Orue-Extebarria J.I., Baceta A., Payros A., Larruzea I.F. 2000. Uppermost Cretaceous-Middle Eocene strata of the Basque-Cantabrian region and western Pyrenees: a sequence stratigraphic perspective. Revista de la Sociedad Geológica de España 13, 191-211.

Pujalte V., Baceta J.I., Schmitz B. 2015. A massive input of coarse-grained siliciclastics in the Pyrenean Basin during the PETM: the missing ingredient of a coeval abrupt change in hydrological regime. Climate of the Past, Discussions 11, 2889-2931.

Remacha E., Fernandez L.P., Maestro E., 2005. The transition between sheet-like lobe and basin plain turbidites in the Hecho basin (south-central Pyrenees, Spain). Journal of Sedimentary Research 75, 789-819.

Ravenne C., Beghin P., 1983. Apport des experiences en canal à l'interprétation sédimentologique des depots de cones détritique sous-marins. Institut Francais du Petrole, Reveu 38, 279-297.

Ricci Lucchi F., 1981. The Marnoso-arenacea turbidites, Romagna and Umbria Apennines. In: Ricci Lucchi F. (Ed.), Excursion Guidebook, with Contribution on Sedimentology of Some Italian Basins. 2nd IAS European Meeting, Bologna, 229-303.

Salinas J., Balachandar S., Shringarpure M., Cantero M., 2020. Soft transition between subcritical and supercritical currents through intermittent cascading interfacial instabilities. Proceedings of the National Academy of Sciences (PNAS) 117, 18278-18284.

Sanders J.E., 1965. Primary sedimentary structures formed by turbidity currents and related resedimentation mechanisms. In: Middleton G.V. (Ed.), Primary Sedimentary Structures and Their Hydrodynamic Interpretation. SEPM, Special Publication 12, 192-219.

Scacchia E., Tinterri R., Gamberi F., 2022a. The influence of channel planform and slope topography on turbidity current overbank processes: the example of the Acquarone Fan (Southeastern Tyrrhenian Sea). Frontiers in Earth Science 9, 785164.

Scacchia E., Gamberi F., Fedele J., Tinterri R., 2022b. Short-distance facies changes related to a lateral bounding slope (Marnoso-arenacea Formation, Italy). SEPM Bouma Virtual Conference, 20-22 April 2022, Abstract book, p. 21.

Scacchia E., Tinterri R., Gamberi F., 2024. Downslope evolution of supercritical bedforms in a confined deep-sea fan lobe, Amantea Fan, Paola Basin (Southeastern Tyrrhenian Sea). Sedimentary Geology 466, 106636.

Sequeiros O.E., 2012. Estimating turbidity current conditions from channel morphology: A Froude Number approach. Journal of Geophysical Research, Oceans 117, 1-19.

Sequeiros O.E., Spinewine B., Parker G., Pirmez C., Viparelli E, Fedele J., García M.H., Koller D., Pittaluga M.B., Yokokawa M., 2026. Regimes of bedforms created by down-slope density currents. Earth-Science Reviews 272, 105322.

Simons D.B., Richardson E.V., Nordin C.F.Jr., 1965. Sedimentary structures generated by flow in alluvial channel. In: Middleton G.V., Bouma A.H. (Eds.), Turbidites and Deep-Water Sedimentation: Pacific Section SEPM, Los Angeles, California, 34-52.

Slootman A., 2020. Supercritical flows: bedforms of the illustrious upper flow-regime. Seds Online presentation, 4 November, 2020, https://sedsonline.com/webinar_

category/scientific-webinars/.

Slootman A., Cartigny M.J.B., 2020. Cyclic steps: review and aggradation-based classification. Earth-Science Reviews 201, 102949.

Slootman A., Ventra D., Cartigny M.J.B., Normandeau A., Hubbard S., 2021. Supercritical-flow processes and depositional products: introduction to thematic issue. Sedimentology 68, 1289-1296.

Sohn Y.K., 1997. On traction-carpet sedimentation. Journal of Sedimentary Research 67, 502-509.

Sumner E.J., Peakall J., Parsons D.R., Wynn R.B., Darby S.E., Dorrell R.M., McPhail S.D., Perrett J., Webb A., White D., 2013. First direct measurements of hydraulic jumps in an active submarine density current. Geophysical Research Letters 40, 5904-5908.

Tagliaferri A., Tinterri R., Pontiggia M., Da Pra A., Davoli G., Bonamini E., 2018. Basin-scale, high-resolution three-dimensional facies modeling of tectonically confined turbidites: an example from the Firenzuola system (Marnoso-arenacea Formation, northern Apennines, Italy). American Association of Petroleum Geologists Bulletin 102, 1601-1626.

Talling P.J., Masson D.G., Sumner E.J., Malgesini G., 2012. Subaqueous sediment density flows: depositional processes and deposit types. Sedimentology 59, 1937-2003.

Taylor W.J., Hodgson D.M., Peakall J., Kane I.A., Morris E., Flint S.S., 2024. Unidirectional and combined transitional flow bedforms: controls on process and distribution in submarine slope settings. Sedimentology 71, 1329-1362.

Tinterri R., 2011. Combined flow and sedimentary structures and the genetic link between sigmoidal and hummocky-cross stratification. GeoActa 10, 43-85.

Tinterri R., 2025. A new turbidite facies-tract scheme including supercritical and transitional sand–mud flows: an outcrop perspective from Mediterranean-type foreland basins. Journal of Sedimentary Research 95, 239-272.

Tinterri R., Civa A., 2021. Laterally accreted deposits in low efficiency turbidites associated with a structurally-induced topography (Oligocene Molare Group, Tertiary Piedmont Basin, NW Italy). Journal of Sedimentary Research 91, 751-772.

Tinterri R., Muzzi Magalhaes P., 2011. Synsedimentary structural control on foredeep turbidites: an example from Miocene Marnoso–arenacea Formation, Northern Apennines, Italy. Marine and Petroleum Geology 28, 629-657.

Tinterri R., Piazza A., 2019. Turbidites facies response to the morphological confinement of a foredeep (Cervarola Sandstones Formation, Miocene, northern Apennines, Italy). Sedimentology 66, 636-674.

Tinterri R., Tagliaferri A., 2015. The syntectonic evolution of foredeep turbidites related to basin segmentation: facies response to the increase in tectonic confinement (Marnoso–arenacea Formation, Miocene, Northern Apennines, Italy). Marine and Petroleum Geology 67, 81-110.

Tinterri R., Drago M., Consonni A., Davoli G., Mutti E., 2003. Modelling subaqueous bipartite sediment gravity flows on the basis of outcrop constraints: first results. Marine and Petroleum Geology 20, 911-933.

Tinterri R., Muzzi Magalhaes P., Tagliaferri A., Cunha R.S., 2016. Convolute laminations and load structures in turbidites as indicators of flow reflections and decelerations against bounding slopes. Examples from the Marnoso–arenacea Formation (northern Italy) and Annot Sandstones (south eastern France). Sedimentary Geology 344, 382-407.

Tinterri R., Laporta M., Ogata K., 2017. Asymmetrical cross-current turbidite facies tract in a structurally-confined mini-basin (Priabonian–Rupelian, Ranzano Sandstone, northern Apennines, Italy). Sedimentary Geology 352, 63-87.

Tinterri R., Civa A., Laporta M., Piazza A., 2020. Turbidites and turbidity currents. In: Scarselli N., Jurgen A., Chiarella D., Roberts D.G., Bally A.W., (Eds.), Regional Geology and Tectonics: Principles of Geologic Analysis. 2nd Edition, Elsevier, 441-479.

Tinterri R., Mazza T., Magalhaes P.M., 2022. Contained-reflected megaturbidites of the Marnoso-arenacea Formation (Contessa key Bed) and Helmintoid Flysches (Northern Apennines, Italy) and Hecho Group (South-Western Pyrenees). Frontiers in Earth Science 10, 817012.

Vendettuoli D., Clare M.A., Clarke J.E.H., Vellinga A., Hizzet J., Hage S., Cartigny M J.B., Talling P.J., Waltham D., Hubbard S.M., Stacey C., Lintern D.G., 2019. Daily bathymetric surveys document how stratigraphy is built and its extreme incompleteness in submarine channels. Earth and Planetary Science Letters 515, 231-247.

Van Vliet A., 1982. Submarine fans and associated deposits in the Lower Tertiary of Guipuzcoa (Northern Spain). PhD Thesis, University of Utrech, pp. 145.

Walker R.G., 1967. Upper flow regime bed forms in turbidites of the Hatch Formation, Devonian of the New York State. Journal of Sedimentary Petrology 37, 1052-1058.

Wilkin J., Cuthbertson A., Dawson S., Stow D., Stephen K., Nicholson U., Penna N., 2023. The response of high-density turbidity currents and their deposits to an abrupt channel termination at a slope break: implications for channel-lobe transition zones. Sedimentology 70, 1164-1194.

Wynn R.B., Kenyon N.H., Masson D.G., Stow D.A.V., Weaver P.P. E. 2002. Characterization and recognition of deep-water channel-lobe transition zones. American Association of Petroleum Geologists Bulletin 86, 1441-1462.

Zavala C., Arcuri M., 2016. Intrabasinal and extrabasinal turbidites: Origin and distinctive characteristics. Sedimentary Geology 337, 36-54.